SEVENTH FRAMEWORK PROGRAMME
THEME – ICT
[Information and Communication Technologies]

Contract Number:	223854
Project Title:	Hierarchical and Distributed Model Predictive Control of Large-Scale Systems
Project Acronym:	HD-MPC

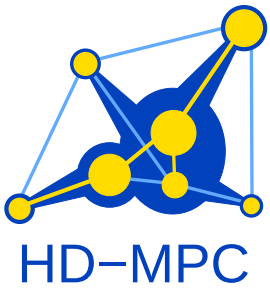

Deliverable Number:	D3.4.2
Deliverable Type:	Report
Contractual Date of Delivery:	December 1, 2010
Actual Date of Delivery:	**November 30, 2010**
Title of Deliverable:	**Report on implementation of timing and delay related approaches to simple case studies**
Dissemination level:	Public
Workpackage contributing to the Deliverable:	WP4
WP Leader:	Wolfgang Marquardt
Partners:	RWTH, TUD, POLIMI, USE, UNC, SUPELEC, UWM
Author(s):	A. Núñez, T.L.M. Santos, D. Limon, J.E. Normey-Rico, T. Alamo, J. Espinosa, F. Valencia, A. Marquez, J. Lopez, J. Garcia, Y. Li, B. De Schutter

Table of contents

Project co-ordinator

Name: Bart De Schutter
Address: Delft Center for Systems and Control
Delft University of Technology
Mekelweg 2, 2628 Delft, The Netherlands
Phone Number: +31-15-2785113
Fax Number: +31-15-2786679
E-mail: b.deschutter@tudelft.nl
Project web site: `http://www.ict-hd-mpc.eu`

Executive Summary

In this report, timing and delay related approaches are implemented to three simple case studies: a four-tank process, a laboratory heater process, and irrigation channels. The approaches explicitly deal with timing and delay issues, and to compute the control actions a centralized model predictive controller (MPC), a robust MPC, and a distributed controller are used, according to the most suitable scheme for each case study. The report is divided as follows:
In Chapter 1 a synopsis of the report is presented, where the main results of the subsequent chapters can be found, as well as their importance for HD-MPC as a whole.
In Chapter 2, an approach to deal with the loss of performance when measurements have a delay due to communication over networks is presented. The delay is allowed to vary randomly, and the estimation of the states is obtained by using a moving horizon estimator (MHE) with variable structure. A centralized model predictive controller (MPC) is used to compute the control actions. The resulting pair MHE-MPC is tested using the four-tank process, and the simulation results show a good performance of the approach.
In Chapter 3, the explicit compensation effect is discussed in a robust context. The conditions to guarantee robust stability and robust constraint satisfaction, in the presence of additive state disturbances, are presented. A robust tube MPC is applied to guarantee these conditions and a first-order plus dead-time (FOPDT) model is considered to take some advantages of the proposed explicit compensation MPC scheme. Finally the experimental case study used is a laboratory heater process, and some properties of the proposed algorithm are discussed.
Lastly, in Chapter 4, a distributed control scheme that inherits the interconnection structure of a string of pools with distant-downstream control is studied. It is shown that the internal time-delay for water transport from upstream to downstream not only limits the local control performance of regulating water-levels at set-points and rejecting off-take disturbances in each pool, but also impacts the global performance of managing the water-level error propagation and attenuating the amplification of control actions in the upstream direction. The decoupling terms in the distributed controller helps to improve global closed-loop performance by decreasing the low-frequency gain of the closed-loop coupling. Moreover, they compensate for the influence of the time-delay by imposing extra phase lead-lag compensation in the mid-frequency range on the closed-loop coupling function.

Chapter 1

Synopsis of the Report

1.1 Introduction

When a control system is implemented in a hierarchical or in a distributed fashion, with multiple processors communicating over a network, both the communication delays associated with the network and the computation delays associated with the processing time can degrade the performance of the system. In this case, the performance of the system may depend not only on the performance of the individual components but also on their interaction and cooperation, [45]. A recent literature survey and analysis regarding timing and delay issues can be found in [23].

In this report, timing and delay related approaches are implemented to three simple case studies. The approaches explicitly deal with timing and delay issues, and to compute the control actions in Chapter 2 a centralized model predictive controller (MPC) is used to control a four-tank process, in Chapter 3 a robust MPC to control a laboratory heater process, and in Chapter 4 a distributed controller for irrigation channels.

The aim of this first chapter is to provide to the reader an insight of the main results of this report. The interested reader can then find more details in the subsequent chapters.

1.2 Variable delay compensation using moving horizon estimation in model predictive control schemes

When measurements are transmitted from networked sensors to the control system using communication networks a variable transport delay appears due to communication problems such as: congestion, noisy environments, error correction sequences, variable routing paths, etc. These delays can cause deterioration of the performance of the control system. In some cases these variable communication paths can cause that data measured at time instant k is received after the data measured at time $k+d$ where $d > 0$, meaning that data arrives to the controller not only with delay but also in a non-correct sequence.

Dealing with such challenging situation demands the use of a state observer capable of accommodating large data sequences received at a non-regular basis in order to estimate correctly the states in spite of the delays. The only observer strategy with a natural capability to accommodate such irregular sampling is the Moving Horizon Estimation (MHE) observer. The MHE is a well-known model-based technique that performs a nonlinear optimization in order to estimate the states of the systems taking into account the physical constraints on the states, measurements, and inputs [14, 29, 35].

In order to deal with the variable transport delay conditions, in Chapter 2 we propose the use of MHE to estimate the states with the available data organized in stacks while updating the state covariance matrix penalizing only the estimation errors for the available data. Despite of the advantages of the MHE, if the delay on the measurements is not properly handled, the performance of the estimation may fall. Consequently, a procedure to handle the delays in this type of estimators is developed. As a simple case study, in order to verify the proposed methodology, a quadruple tank process is considered. In the simulations, the performance of a pair MHE-MPC is evaluated with and without the new proposed MHE with variable structure procedure to tackle the problem of the delay in the measurements of the states.

Assume that a linear model can be derived from the linearization of a non-linear large-scale system, around each operating point. The linear model is given by:

$$\begin{aligned} \hat{x}(k+1) &= A(k)\hat{x}(k) + B(k)u(k) + G(k)w(k) \\ \hat{y}(k) &= C(k)\hat{x}(k) + v(k) \end{aligned} \tag{1.1}$$

where $\hat{x}(k) \in \mathbb{R}^n$ and $w(k) \in \mathbb{R}^w$ are the linearized state and uncertainty respectively, $v(k) \in \mathbb{R}^p$ is the linearized measurement noise, and $u(k) \in \mathbb{R}^m$ denotes the system input. Moreover, these variables are constrained as shown in (2.2). Thus, the estimation of the whole state can be formulated as an MHE problem as follows:

$$\Phi_k^* = \min_{x_0, \{w_j\}_{j=0}^{k-1}} \Phi_k(x_0, \{w_j\}_{j=0}^{k-1}) \tag{1.2}$$

with x_0 being the initial state. The problem is subject to the following constraints:

$$x_j \in \mathbb{X} \text{ for } j = 0, \ldots, k,\ w_j \in \mathbb{W} \text{ for } j = 0, \ldots, k-1,$$

and the cost function is:

$$\Phi_T(x_{T-N}, \{w_k\}_{k=T-N}^{T-1}) = \sum_{k=T-N}^{T-1} \|y(k) - \hat{y}(k)\|_Q^2 + \|w(k)\|_R^2 \tag{1.3}$$

where N is the horizon of the MHE. In the context considered here, it is necessary to make a correction to the traditional MHE scheme in order to assure that the estimator calculates the appropriate value of the states when the measurements are delayed. With this purpose, a variant of the MHE is proposed.

Let $\widetilde{y}(k)$ denote the sequence of available measurements at time step k. Let $\widetilde{d}(k)$ denote the sequence containing the delay associated with each measurement in $\widetilde{y}(k)$. The sequence $\widetilde{y}(k)$ may not contain all the measurements on the window of the MHE because some data have not yet arrived due the delay, or may not arrive at all.

Assume that the delay of each measurement belonging to $\widetilde{y}(k)$ is known and is randomly distributed. With the sequence of delays it is possible to neglect some terms of the cost function, since there is no data available to compare the estimated and the measured value. With this approach the MHE problem becomes a variable structure problem, in which the length of the sequence of available measurements and the dimension of the weighting matrix Q change at each time step k accordingly with the available measurements.

So, the expression for computing the estimated output $\overline{y}(k)$ becomes

$$\overline{y}(k) = \begin{bmatrix} \Gamma^{N-d_1} \\ \vdots \\ \Gamma^{N-d_n} \end{bmatrix} x(k-N) + \begin{bmatrix} \Xi^{N-d_1} \\ \vdots \\ \Xi^{N-d_n} \end{bmatrix} \widetilde{u}(k) \tag{1.4}$$

where $\{d_1,\ldots,d_n\}$ is the sequence of the delays, $\Gamma^i = CA^i$, $\Xi^i = [CA^{i-1}B,\ldots,CB]$, $\widetilde{u}(k) = [u^T(k-N),\ldots,u^T(k-1)]^T$. Hence the cost function (1.3) becomes:

$$\Phi_T(x_{T-N},\{w_k\}_{k=T-N}^{T-1}) = \sum_{k=T-N}^{T-1} \|\tilde{y}(k)-\overline{y}(k)\|_Q^2 + \|w(k)\|_R^2 \tag{1.5}$$

In order to implement the proposed MHE, the following steps are suggested:

1. Given the sequence of measurements $\{y(k-N),\ldots,y(k-1)\}$, and the sequence of delays $\{d(k-N),\ldots,d(k-1)\}$, arrange the vector of measurements, where each measurement position is given by $\frac{d(k-l)}{T_s}$.
2. With the arranged vector of measurements, identify which block of the matrix Q should be neglected.
3. Estimate the states according to the MHE.
4. After computing the estimated value of the states, send them to the controller and go back to step 1.

Next, we compare the performance of the pair MHE-MPC on a four-tank process proposed by [16], with and without considering the proposed variable structure in the MHE, using a random normally distributed delay on the measurements.

The target in the system is to regulate the level of the tanks 1 and 2, by modifying the flows q_a and q_b feeding the tanks. In this case we consider as manipulated variables the flows q_a and q_b, as controlled variables the levels h_1 and h_2, and as estimated variables the levels h_3 and h_4. A diagram and the equations of the system can be found in Chapter 2. In order to test the proposed MHE, three cases were considered: the measurements of the states were taken without delay, the measurements of the states were taken with delay and a fixed structure MHE was implemented and, the measurements of the states were taken with delay and the proposed MHE was implemented.

When there was no delay in the measurement of the states, the values of the states given by the MHE converge to their real values. The pair MHE-MPC is able to lead the controllable variables of the system to their desired values, despite of the changes on the set-point. After the convergence of the MHE the values of the states estimated by the MHE are the same as their real values. But, if a time delay is included in the measurements of the states, the performance of the system decreases. Despite of the convergence of the MHE, the pair MHE-MPC is not able to lead the controllable variables to their set-point.

In order to avoid the effects of the delay on the system, the proposed MHE was implemented. In this case, the value of the estimates reached the real values despite of the random delay and the changes in the set-points of the controllable variables. In comparison with the behavior of the system without delay, with the initial set-point one can observe an expected delay on the convergence of the controllable variables to their reference values, due to the lack of available data for the state estimation. The proposed variable structure MHE neglected the random delay conditions. However, the control actions computed by the MPC under random delay conditions and with the proposed variable structure MHE, were larger in amplitude compared with the control actions without delay and fixed structure MHE.

As conclusions of this work, under the same conditions, the proposed MHE improved the performance of the pair MHE-MPC, exhibiting a performance similar than the pair MHE-MPC without delay. Then, it is possible to conclude that the MHE with variable structure proposed on this work neglects the effect of the random delay on the measurements.

1.3 On the explicit dead-time compensation in robust MPC. Application to a laboratory heater process

Intrinsic dead-time compensation is one of the advantages of model predictive control (MPC) [5]. However, stability of the MPC schemes is related to a terminal cost, a terminal set, and a stabilizing control law [26] which are usually derived from a delay-free model. Dead-time compensation schemes have been known in the control community since Smith's seminal work [41]. In general, dead times are not considered to be a problem for MPC strategies due to the intrinsic compensation property.

Following the ideas of [38, 39], a robust explicit dead-time compensation for constrained linear systems with additive disturbances will be presented. Additionally, a robust MPC for tracking will be particularized for first-order plus dead-time models (FOPDT/IPDT) [39] in order to take some advantages of the proposed compensation scheme, deriving a simple explicit robust control law (see more details in Chapter 3).

Now, the explicit compensation effect will be analyzed in terms of a state additive disturbance in order to consider robust stability and constraint satisfaction. Hence, the real dynamic is represented by

$$x(k+1) = Ax(k) + Bu(k-d) + w(k). \tag{1.6}$$

with $x(k)$ the state, $u(k)$ the input, $w(k) \in \mathbb{W}$ where $\mathbb{W}$ is a compact polytope that contains the origin. It is important to emphasize that the effect of noise, external unmeasured disturbances and process-model mismatches (including dead-time estimation uncertainty) appears in $w(k)$. A simple idea, discussed in [36], can be applied to consider a prediction model without dead-time. From the model it can be observed that there is no effect of $u(k)$ over $x(k+1|k)$, $x(k+2|k)$, ..., $x(k+d|k)$ due to the dead-time. As a consequence, $x(k+d|k)$ depends only on past controls so that it can be obtained recursively by using

$$x(k+d|k) = A^d x(k) + \sum_{j=1}^{d} \left[A^{j-1} B u(k-j)\right]. \tag{1.7}$$

A new controlled state can be defined as

$$\tilde{x}(k) \triangleq x(k+d|k) \tag{1.8}$$

Then, by considering the explicit compensation scheme, the predicted behavior can be described by

$$\tilde{x}(k+1) = A\tilde{x}(k) + Bu(k) + \tilde{w}(k) \tag{1.9}$$

where $\tilde{w}(k)$ is the effect of $w(k)$ on the predicted state ($\tilde{x}(k)$).

In Chapter 3 it is shown that for a given system, $\tilde{w}(k)$ is uniquely determined by $w(k)$:

$$\tilde{w}(k) = A^d w(k), \tag{1.10}$$

so that for $w(k) \in \mathbb{W}$, $\tilde{w}(k) \in A^d\mathbb{W} \triangleq \tilde{\mathbb{W}}$.

If there are constraints on the state, it is necessary to guarantee robust constraint satisfaction of $x(k)$ instead of $\tilde{x}(k)$. Thus, prediction error should be analyzed once $\tilde{x}(k)$ is the variable used for control purposes. The following prediction error expression can be obtained (see details in Chapter 3):

$$e(k) = A^{d-1}w(k-d) + A^{d-2}w(k-d+1) + \cdots + w(k-1). \tag{1.11}$$

then the prediction error may be bounded by

$$\mathbb{E} = A^{d-1}\mathbb{W} \oplus A^{d-2}\mathbb{W} \oplus \cdots \oplus \mathbb{W}. \tag{1.12}$$

Similarly to [25], once the error is bounded, it can be concluded that if

$$\tilde{x}(k) \in \mathbb{X} \ominus \mathbb{E},\ \forall k \geq 0 \Rightarrow x(k) \in \mathbb{X},\ \forall k \geq d.$$

Note that $\mathbb{E}$ is also a compact polytope that contains the origin.

Now, the explicit compensation effect will be considered in the context of a general control law $\kappa(\cdot)$ formulated in terms of the following Lemma, that allows to analyze robustness and constraint satisfaction.

Lemma. 1

(i) *Let $u(k) = \kappa(\tilde{x}(k))$ be a control law such that*

$$\tilde{x}(k+1) = A\tilde{x}(k) + Bu(k) + \tilde{w}(k)$$

is input-to-state stable (ISS) with $\tilde{w}(k) \in A^d\mathbb{W}$ and F_∞ be its minimum robust positively invariant set.

(ii) *Let*

$$x(k+1) = Ax(k) + B\kappa(\tilde{x}(k-d)) + w(k)$$

be a system with $w(k) \in \mathbb{W}$, $\mathbb{E} = \bigoplus_{j=1}^{d} A^{j-1}\mathbb{W}$ and

$$\tilde{x}(k-d) = A^d x(k-d) + \sum_{j=1}^{d} \left[A^{j-1}Bu(k-j-d)\right].$$

Then:

(a) *System (ii) is input-to-state stable for $\forall w(k) \in \mathbb{W}$ and $\sigma(x(k), F_\infty \oplus \mathbb{E}) \to 0$. Moreover, if $w(k) \to 0$, $x(k) \to 0$;*

(b) *If $\tilde{x} \in \mathbb{X} \ominus \mathbb{E}$, $\forall k \geq 0$, then $x(k) \in \mathbb{X}$, $\forall k \geq d$.*

Qualitatively, it is possible to guarantee that the system without dead-time is constrained to $\tilde{x}(k) \in \mathbb{X} \ominus \mathbb{E}$, $k \geq 0$, then the real state is such that $x(k) \in \mathbb{X}$, $k \geq d$. This result is somehow general because the law $u(k) = \kappa(\tilde{x}(k))$ is not defined. As a consequence, robust MPC schemes are natural candidates to guarantee the conditions. In order to ensure that conditions (i) and (ii) holds, we will consider the tracking problem [22], explained next.

Consider the following uncertain system

$$x^+ = Ax + Bu + w, \quad y = Cx \tag{1.13}$$

where $x \in \mathbb{R}^n$ is the current state, x^+ is the successor state, $u \in \mathbb{R}^m$ is the current control $w \in \mathbb{R}^n$ is an unknown disturbance and $y \in \mathbb{R}^p$ is a desired linear combination of the states. In this case: $x = \tilde{x}(k)$, $x^+ = \tilde{x}(k+1)$ $w = \tilde{w}(k)$, and $y = y(k+d|k)$ subject to compact and convex polyhedral constraints

$$x \in \mathbb{X} \ominus \mathbb{E} \subset \mathbb{R}^n, \quad u \in \mathbb{U} \subset \mathbb{R}^m \tag{1.14}$$

and a disturbance constraint

$$w \in \tilde{\mathbb{W}} \subset \mathbb{R}^n.$$

As proposed in [22], the overall objective is to stabilize the constrained system and steer the state to a neighborhood of the set-point fulfilling the constraints for any possible disturbance. For doing that, a robust MPC strategy based on the notion of tubes and robust positive invariance is considered.

In the robust tube based MPC for reference tracking, the initial nominal state ($\bar{x}(0)$), the nominal sequence of future control action ($\bar{\mathbf{u}}$) and the parameter $\bar{\theta}$, which defines $(\bar{x}_s, \bar{u}_s)$, are decision variables. The cost function is given by

$$V(x, y_r; \mathbf{u}, \bar{x}, \bar{\theta}) = \sum_{i=0}^{N-1} ||\bar{x}_i - \bar{x}_s||_Q^2 + ||\bar{u}_i - \bar{u}_s||_R^2 + ||\bar{x}_N - \bar{x}_s||_P^2 + V_o(\bar{y}_s - y_r).$$

where $\bar{x}_i$ denotes the prediction of $\bar{x}$ i-samples ahead, $(\bar{x}_s, \bar{u}_s) = M_\theta \bar{\theta}$ characterizes the artificial stationary point, $\bar{y}_s = C\bar{x}_s$ is an admissible artificial set-point, y_r is the desired reference for y and $V_o(\bar{y}_s - y_r)$ is an off-set cost [9]. Therefore, the following optimization problem should be solved at each sampling instant

$$\begin{aligned} \min_{\bar{x}(0), \bar{\mathbf{u}}, \bar{\theta}} \quad & V(x, y_r; \bar{x}(0), \bar{\mathbf{u}}, \bar{\theta}) \\ \text{s.t.} \quad & \\ & \bar{x}_0 \in x \oplus (-\mathscr{Z}) \\ & \bar{x}_i \in \mathbb{X} \ominus \mathbb{E} \ominus \mathscr{Z}, \quad i = 0, 1, ..., N-1 \\ & \bar{u}_i \in \mathbb{U} \ominus K\mathscr{Z}, \quad i = 0, 1, ..., N-1 \\ & (\bar{x}_N, \bar{\theta}) \in \Omega_{t,\bar{K}}. \end{aligned}$$

where Ω_{t,K_Ω} is an extended invariant set for tracking by using a given stabilizing controller K_Ω. Finally, The MPC control law is

$$K_{MPC}(x, y_r) = \bar{u}^*(0; x, y_r) + K(x - \bar{x}^*(x, \bar{\theta}))$$

where $\bar{u}^*(0; x, y_r)$ is the first element of the optimal nominal control sequence ($\bar{\mathbf{u}}$) and $\bar{x}^*$ is the optimal nominal value for $x(0)$. The interested reader can see in Chapter 3 the additional assumptions on the MPC parameters to guarantee stability.

In the presence of persistent disturbance, an undesired error will appear because the stationary point parameterization does not consider this disturbance. In this case, a modified reference $y_r^m(k)$ may defined by

$$y_r^m(k) = y_r - y_s^w(k) = y_r - M\hat{w}(k)$$

where $M \in \mathbb{R}^{p \times n}$ is a constant matrix and $\hat{w}(k)$ is an estimation of $w(k)$. If the disturbance estimator is stable and converges to $\hat{w}(k) = w(\infty)$, then $y(k)$ will converge to y_r if it is admissible. Due to separation principle, if $\hat{w}(k) \in \mathbb{W}$, this outer loop does not affect stability because constant disturbance estimation in not related with MPC control law.

The proposed robust tube based MPC will be particularized to discrete FOPDT models. This is motivated by some reasons: these kind of models are common in practice, it becomes much easier to analyze and to obtain the invariant sets, it is not necessary to consider state-estimation and the discussions about dead-time compensator effect becomes more intuitive [39].

Now, consider a model given by

$$P(z) = \frac{k_p}{z - a} z^{-d}$$

and a dead-time free state-space representation (A,B,C,D) with $A=[a]$, $B=[k_p]$, $C=1$ and $D=0$. In this case, the stationary point parameterization can be defined in such a way that θ is the desired reference ($\theta = y_r$) with $M_\theta = [1\ (1-a)/k_p]'$ and $N_\theta = 1$.

Now, it will be considered that the feedback law is in the form $K=(b-a)/(k_p)$ in such a way that $A+BK=b$ with $0 \leq b < 1$, the constraints are $\mathbb{U}=\{u : u_{min} \leq u \leq u_{max}\}$, $\mathbb{X}=\{x : x_{min} \leq x \leq x_{max}\}$ and the disturbance is in the interval $\mathbb{W}=\{w : w_{min} \leq w \leq w_{max}\}$. In this case, the disturbance effect is given by:

$$\begin{aligned}\mathscr{Z} &= a^d\mathbb{W} \oplus ba^d\mathbb{W} \oplus b^2a^d\mathbb{W} \oplus b^3a^d\mathbb{W} \oplus ... \\ &= \left\{\zeta : \frac{a^d}{1-b}w_{min} \leq \zeta \leq \frac{a^d}{1-b}w_{max}\right\}; \end{aligned} \tag{1.15}$$

$$\begin{aligned}\mathbb{E} &= \mathbb{W} \oplus a\mathbb{W} \oplus a^2\mathbb{W} \oplus ... \oplus a^{d-1}\mathbb{W} \\ &= \left\{\varepsilon : \frac{(1-a^d)}{1-a}w_{min} \leq \varepsilon \leq \frac{(1-a^d)}{1-a}w_{max}\right\}. \end{aligned} \tag{1.16}$$

As it was already pointed out that for stable processes the smaller $\mathscr{Z}$ is, the larger the delay is. As consequence, the nominal control constraint, $\overline{\mathbb{U}}$, is larger. However, in the case of the nominal constraint on the state (output), it can be shown that $\overline{\mathbb{X}}$ gets smaller for longer delays only if the closed loop response is slower then open-loop one. In general ($b < a$), the longer the delay is, the larger the prediction error bound is, which makes it more difficult to guarantee state (output) constraints satisfaction.

A laboratory heater process case study is considered. In this system, it is desired to control the temperature in the outlet side of a tube. A constant air stream is used to transfer heat from the heater to the output of the tube where there is a thermistor. An input tension is used to adjust the power dissipated in the heater meanwhile an output tension is used to obtain the temperature information. Both input and output tensions have the same range. In order to emulate input disturbances, the air stream flow can be manually modified.

Simulated results with the nominal model are obtained first. These results are useful to illustrate the robust tube idea: at each sampling instant, the optimal nominal value of the prediction ($\bar{y}^*(k+d|k)$), which may be different from the prediction ($y(k+d|k)$), is protected by an inner and an outer intervals. The smaller one would be enough to guarantee that $y(k+d|k)$ respect the constraints but, the larger one is imposed to ensure that the real future output respect the constraints. Due to the fact that $y(k+d|k)$ is considered for control purposes, it is necessary to consider just the smaller interval to ensure control constraint satisfaction and recursive feasibility (robust stability).

Constant unmeasured disturbances are inserted in the control. The simulation results illustrate that: (i) this algorithm is not conservative in the case of constant disturbances and (ii) constraint satisfaction may be violated if the external interval is not considered.

In the experimental results, disturbances were applied by varying the air stream flow manually. Apart from the noise effect, the results are somehow similar to the simulated case. It is interesting to observe that disturbance dynamics varied naturally during the process operation. It should be also noticed that disturbance variance changed during the process operation but this effect does not affect control signal due to the disturbance estimation filter. Moreover, constant disturbance rejection was properly performed as expected.

1.4 Stability and performance analysis of irrigation channels with distributed control

In irrigation systems water is drawn from a reservoir and distributed through the main channel and many secondary channels to farms. Along the channels, mechanical gates are installed to regulate the flow. A stretch of water between two neighboring gates is called a pool. An irrigation network is often gravity-fed (i.e. there is no pumping); to satisfy water-demands from farms and to decrease water wastage, the water-levels in the pools should be regulated to certain setpoints. To avoid the excessive communication load for large-scale system, decentralized control is preferred to centralized control. The control objectives for large-scale irrigation network involve: locally, setpoints regulation, rejection of off-take disturbances, avoiding excitement of dominant waves and, globally, management of the water-level error propagation and attenuation of the amplification of control action in the upstream direction.

One big issue in control design for an irrigation network comes from the time-delay in each pool, i.e. the time for transporting water from the upstream gate to the downstream gate. In Chapter 4, the impact of the internal time-delays on the local and global control performance is analyzed. Further, we discuss how the distributed control scheme compensates for such impact. Although the chapter focuses on irrigation networks, the discussion can be extended to many practical networks that involve internal time-delay.

A simple model of the water-level in pool$_i$ can be obtained by conservation of mass [6, 43]:

$$\alpha_i \dot{y}_i(t) = u_i(t-\tau_i) - v_i(t) - d_i(t),$$

where u_i is the flow over the upstream gate, v_i the flow over the downstream gate, d_i models the off-take load-disturbances from pool$_i$; τ_i is the transport delay of water from upstream gate to downstream gate of the pool, and α_i a measure of the pool surface area. Taking the Laplace transform, yields

$$P_i:\ y_i(s) \quad = \quad \frac{1}{s\alpha_i}\left(e^{-s\tau_i}u_i - v_i - d_i\right)(s). \tag{1.17}$$

where P_i is the nominal model for pool$_i$. Some of the notations that will be used are: the variable K_i is split into a loop-shaping weight W_i and a compensator K_{∞_i}, y_i^K and u_i^K are input from and output to the shaped plant, respectively. Designing of the distributed controller consists of the following three steps, which are consistent with the well-known $\mathscr{H}_\infty$ loop-shaping approach [28].

1. Design W_i to shape P_i based on local performance. Typical off-takes d_i are step disturbances; based on the internal model principle [13], a simple selection could be $W_i = \frac{\kappa_i}{s}$ for zero steady-state water-level error. For robust stability, κ_i is selected such that the local crossover frequency $\omega_{c_i} \leq 1/\tau_i$ (see [40]). Denote $z_i := \left(e_i, u_i^K\right)^T$ and $n_i := (r_i, \Delta u_i, d_i)^T$, with r_i the water-level setpoint and Δu_i modeling additional uncertainty in flow over gate$_i$. For a channel of N pools, Let $G_s := (G_{s_1}, \ldots, G_{s_N})$ denote the interconnection of the shaped plant

$$G_{s_i} := \begin{pmatrix} v_i \\ n_i \\ u_i^K \end{pmatrix} \mapsto \begin{pmatrix} w_i \\ z_i \\ y_i^K \end{pmatrix}$$
$$= \begin{bmatrix} 0 & (0\ 1\ 0) & 1 \\ \begin{pmatrix} \frac{1}{s\alpha_i} \\ 0 \end{pmatrix} & \begin{pmatrix} 1 & \frac{e^{-s\tau_i}}{-s\alpha_i} & \frac{1}{s\alpha_i} \\ 0 & 0 & 0 \end{pmatrix} & \begin{pmatrix} \frac{e^{-s\tau_i}}{-s\alpha_i} \\ 1 \end{pmatrix} \\ \frac{W_i}{s\alpha_i} & \left(W_i \ \frac{e^{-s\tau_i}W_i}{-s\alpha_i} \ \frac{W_i}{s\alpha_i}\right) & \frac{e^{-s\tau_i}W_i}{-s\alpha_i} \end{bmatrix}$$

   with $v_i = w_{i+1}$ and boundary condition $v_N = 0$. Note that such a boundary condition is possible with distant-downstream control.

2. Synthesize K_{∞_i} to cope with the tradeoff between local performance and closed-loop coupling. Let $K_\infty := (K_{\infty_1}, \ldots, K_{\infty_N})$ denote the interconnection of

$$K_{\infty_i} \quad := \quad \begin{pmatrix} v_i^K \\ y_i^K \end{pmatrix} \mapsto \begin{pmatrix} w_i^K \\ u_i^K \end{pmatrix}$$

with $v_i^K = w_{i+1}^K$ and boundary condition $v_N^K = 0$; and let $H(G_s, K_\infty)$ denote the closed-loop transfer function from $(n_1, \ldots, n_N)^T$ to $(z_1, \ldots, z_N)^T$. The synthesis problem is formulated as

$$\begin{aligned} &\min_{K_\infty \in \mathscr{K}_{\text{syn}}} \ \gamma \\ &\text{subject to} \\ &\|H(G_s, K_\infty)\|_\infty \ < \ \gamma \end{aligned} \tag{1.18}$$

where $\mathscr{K}_{\text{syn}}$ represents the set of stabilizing K_∞'s. Note that we use $\|\cdot\|_\infty$ to denote the $\mathscr{H}_\infty$ norm of a transfer function. Such a structured optimization problem can be solved by employing the technique in [19], see [20].

3. The final distributed controller is then given by

$$K_i \quad := \quad \begin{pmatrix} v_i^K \\ e_i \end{pmatrix} \mapsto \begin{pmatrix} w_i^K \\ u_i \end{pmatrix} = K_{\infty_i} \begin{bmatrix} 1 & 0 \\ 0 & W_i \end{bmatrix}.$$

For distant-downstream control, the internal time-delay τ_i limits the local performance. For example, the local bandwidth limit of $1/\tau_i$ is previously considered in the selection of the weight gain, κ_i. In this section, the influences of τ_i on the closed-loop coupling are discussed. It is shown that such time-delays, not only make it difficult to manage the water-level error propagation, but also cause the amplification of control action, in the upstream direction. Further, analysis is made on how the distributed control compensates for such influences.

For a channel of N pools

$$\begin{aligned} \begin{pmatrix} y_1 \\ \vdots \\ y_{N-1} \\ y_N \end{pmatrix} \quad &= \quad \begin{bmatrix} G_1 & \tilde{G}_1 & & \\ & \ddots & \ddots & \\ & & G_{N-1} & \tilde{G}_{N-1} \\ & & & G_N \end{bmatrix} \begin{pmatrix} u_1 \\ \vdots \\ u_{N-1} \\ u_N \end{pmatrix} \\ &+ \quad \begin{bmatrix} \tilde{G}_1 & & \\ & \ddots & \\ & & \tilde{G}_N \end{bmatrix} \begin{pmatrix} d_1 \\ \vdots \\ d_N \end{pmatrix} \end{aligned} \tag{1.19}$$

where $G_i = \frac{1}{s\alpha_i} e^{-s\tau_i}$ and $\tilde{G}_i = -\frac{1}{s\alpha_i}$. It is reasonable to assume $v_N = 0$ as boundary condition for synthesis of the distributed controller under distant-downstream control. The distributed controller is represented by

$$\begin{aligned} K_1 \quad &: \quad u_1 = \begin{bmatrix} K_1^{21} & K_1^{22} \end{bmatrix} \begin{pmatrix} w_2^K \\ e_1 \end{pmatrix} \\ K_i \quad &: \quad \begin{pmatrix} w_i^K \\ u_i \end{pmatrix} = \begin{bmatrix} K_i^{11} & K_i^{12} \\ K_i^{21} & K_i^{22} \end{bmatrix} \begin{pmatrix} w_{i+1}^K \\ e_i \end{pmatrix} \\ &\qquad \text{for } i = 2, \ldots, N-1 \\ K_N \quad &: \quad \begin{pmatrix} w_N^K \\ u_N \end{pmatrix} = \begin{bmatrix} K_N^{12} \\ K_N^{22} \end{bmatrix} e_N \end{aligned}$$

This gives the general form of the distributed controller K:

$$\begin{pmatrix} u_1 \\ \vdots \\ u_N \end{pmatrix} \quad = \quad \begin{bmatrix} K_{11} & \cdots & K_{1N} \\ & \ddots & \vdots \\ & & K_{NN} \end{bmatrix} \begin{pmatrix} e_1 \\ \vdots \\ e_N \end{pmatrix}; \tag{1.20}$$

where for $i = 1, \ldots, N$, $K_{ii} = K_i^{22}$, which takes care of local performance, and the additional decoupling terms

$$\begin{aligned} K_{i,i+1} &= K_i^{21} K_{i+1}^{12}, \\ K_{ij} &= K_i^{21} \left(\prod_{k=i+1}^{j-1} K_k^{11} \right) K_j^{12} \text{ for } j > i+1. \end{aligned} \tag{1.21}$$

Note that $e_i = r_i - y_i$. Then the closed-loop relationship between water-level errors and off-take disturbances is:

$$\begin{pmatrix} e_1 \\ \vdots \\ e_N \end{pmatrix} = \begin{bmatrix} M_{11} & \cdots & M_{1N} \\ & \ddots & \vdots \\ & & M_{NN} \end{bmatrix} \begin{pmatrix} d_1 \\ \vdots \\ d_N \end{pmatrix} \tag{1.22}$$

where for $i = 1, \ldots, N$, $M_{ii} = -\tilde{G}_i \left(1 + G_i K_{ii}\right)^{-1}$ and for $j \geq i+1$

$$M_{ij} = M_{ii} \sum_{k=i+1}^{j} \left(K_{i+1,k} - K_{ik} e^{-s\tau_i} \right) M_{kj}. \tag{1.23}$$

We see that the closed-loop transfer matrix is upper-triangular, hence the multivariable system inherits the local stabilities. That is, the multivariable system is stable *if and only if* all monovariable systems are stable. Since all the lower off-diagonal entries are null, even for model mismatch, robustness is also inherited from local systems. A perfect decoupling is achieved if for all $j > i$,

$$K_{i+1,j} - K_{ij} e^{-s\tau_i} = 0. \tag{1.24}$$

This requires $K_{ij} = K_{i+1,j} e^{s\tau_i}$, which is non-causal and hence impractical.

Next, analysis of global closed-loop performance is made on the two typical coupling properties of a (distant-downstream) controlled irrigation channel: water-level error propagation and amplification of control action. Assume only d_N occurs in the system, while $d_i = 0$ for $i = 1, \ldots, N-1$. Then from (1.22),

$$\begin{aligned} & T_{e_{i+1} \mapsto e_i} := M_{i,N} M_{i+1,N}^{-1} \\ & = M_{ii} (K_{i+1,i+1} - e^{-s\tau_i} K_{i,i+1}) + \\ & M_{ii} \sum_{k=i+2}^{N} \left(K_{i+1,k} - K_{ik} e^{-s\tau_i} \right) M_{kN} \\ & \left(M_{i+1,i+1} \sum_{k=i+2}^{N} \left(K_{i+2,k} - K_{i+1,k} e^{-s\tau_{i+1}} \right) M_{kN} \right)^{-1}. \end{aligned}$$

Small $\|T_{e_{i+1} \mapsto e_i}\|_\infty$ (e.g. $\ll 1$) represents a good management of the water-level error propagation.

The coupling of control actions responding to d_N is

$$T_{u_{i+1} \mapsto u_i} := \sum_{k=i}^{N} K_{ik} M_{kN} \left(\sum_{k=i+1}^{N} K_{i+1,k} M_{kN} \right)^{-1}.$$

The following discussion shows that $\|T_{u_{i+1} \mapsto u_i}\|_\infty > 1$.

For an irrigation channel with purely decentralized feedback control, i.e. K in (1.20) being diagonal, $T_{u_{i+1} \mapsto u_i} = M_{ii} K_{ii} = -\tilde{G}_i K_{ii} \left(1 - \tilde{G}_i K_{ii} e^{-\tau_i s}\right)^{-1}$. Note that $\tilde{G}_i K_{ii}$ involves two integrators. Applying Lemma 9.3 of [13], it is straightforward to prove $\|T_{u_{i+1} \mapsto u_i}\|_\infty > 1$.

Generally, under distant-downstream control (i.e. without the constraints that K in (1.20) be diagonal), to compensate the influence of the internal time-delay, the amplification of control action in the upstream direction is unavoidable.

The synthesis of K_∞ copes with the tradeoff between the local performance and the decoupling of the closed-loop system. To see how the distributed controller compensates for the influence of internal time-delays, we study the time and frequency responses of a string of three pools with distributed control.

The three pools are taken from Eastern Goulburn No 12, Victoria, Australia. The closed-loop coupling term M_{ij} is composed of $M_{ij}^k := M_{ii}\left(K_{i+1,k} - K_{ik}e^{-s\tau_i}\right)M_{kj}$ for $k = i+1,\ldots,j$. Regarding the impact of K_{ik} on M_{ij}^k in the three-pool example, it is observed that:

1. K_{ik} decreases the gain of M_{ij}^k at low frequencies where typical off-take disturbances are significant;

2. K_{ik} operates on M_{ij}^k by imposing on $M_{ii}K_{i+1,k}M_{kj}$ an additional phase lead-lag compensation around the frequency of $1/\tau_i$.

The first observation explains why with K_{ij} operating on the closed-loop, a better management of water-level error propagation is achieved. Although it is difficult to directly make conclusions of global performance from the second observation, time-responses of control actions show that with the K_{ij}'s the closed-loop predicts the influence of the internal time-delays and that the control action in response to off-take disturbance is faster than that without the K_{ij}'s.

The analysis shows that the distributed controller compensates the time-delay influence by decreasing the low-frequency gain of the close-loop coupling term and imposing extra phase lead-lag compensation in the mid-frequency range on the closed-loop coupling term.

Based on the above observations of the function of the decoupling terms of the distributed controller, it is of interest in future research to investigate the involvement of similar components, e.g. phase lead-lag in decentralized feed-forward compensators, in addition to the purely decentralized feedback controller, for a better global closed-loop performance.

Chapter 2

Variable Delay Compensation Using Moving Horizon Estimation in Model Predictive Control Schemes

2.1 Introduction

When measurements are transmitted from networked sensors to the control system using communication networks a variable transport delay appears due to communication problems such as: congestion, noisy environments, error correction sequences, variable routing paths, etc. These delays can cause deterioration on the performance of the control system. In some cases these variable communication paths can cause that a data measured at time instant k is received after the data measured at time $k+d$ where $d > 0$, meaning, data arrive to the controller not only with delay but also in a non-correct sequence.

Dealing with such challenging situation demands the use of a state observer capable of accommodating large data sequences received at a non regular basis in order to estimate correctly the states in spite of the delays. This problem can be seen in a similar way as inferential sensors are used in chemical applications were variable delayed lab samples are used together with regular sample to reconciliate model based predictions. The only observer strategy with a natural capability to accommodate such irregular sampling is the Moving Horizon Estimation (MHE) observer.

The MHE is a well known model based technique used to estimate the states and parameters of a wide variety of plants. It performs a nonlinear optimization in order to estimate the states of the systems taking into account the physical constraints on the states, measurements and inputs [14, 29, 35]. This estimation technique has shown excellent results when used in non-linear processes, where restricted control actions and constrained states are enforced in order to guarantee stability [3, 15].

The finite moving horizon of the MHE is a fixed-size window observer that only takes into account the last N time instants. The window size must guarantee enough information to reconstruct the states while compensating modeling and measurement errors. The size of the window is chosen according to the dynamics of the plant, roughly around the settling time.

In order to deal with the variable transport delay conditions, we propose to organize the incoming data from the sensors into a stack assuming that each package with a measurement includes the time stamp when the measurement was taken. Then the MHE estimates, at each time instant, the states with the available data organized in the stack while updating the state covariance matrix penalizing only the estimation errors for the available data. Then we can say that this methodology applies state

corrections only if the evidence coming from the sensor is telling so. In order to verify the proposed methodology, a quadruple tank process is implemented without and with delay conditions on the state measurements. As a result, the performance of a pair MHE-MPC was evaluated with and without the proposed variable structure MHE.

This Chapter is organized as follows: Section 1 presents the problem statement, Section 2 presents the simulations results, and Section 3 presents the conclusions and future work.

2.2 Problem statement

Moving Horizon Estimation (MHE) strategies were born as a dual problem of the Model Predictive Control (MPC). Despite the similarities among MPC and MHE, MPC technology was successfully developed and exploited in oil refining industry, whereas MHE theory remained to be a topic of study in academia with very few industrial applications [1].

The basic strategy of MHE reformulates the estimation problem as a quadratic problem using a moving, fixed-size estimation window. The fixed-size window is needed in order to bind the computational effort to solve an otherwise infinite sized problem. This is the main difference of MHE with the batch estimation problem (or full information estimator) [10, 1, 37]. Once a new measurement is available, the oldest one is discarded, using the concept of window shifting.

The main advantage of MHE in comparison with other estimation schemes (like the Kalman Filter) is the straightforward constraint handling inside the optimization problem, and the possibility to propose a cost function. However, as MHE is a limited memory filter, stability and convergence issues arise. A review on latest developments on MHE procedures was published by García and Espinosa in [12].

Despite of the advantages of the MHE, if the delay on the measurements is not properly handle, the performance of the estimation may fall. Consequently, a procedure or method to handle the delays in this type of estimators should be developed. Below, the MHE is introduced and a procedure to tackle the problem of the delay in the measurements of the states is presented.

2.2.1 Moving horizon estimator

Assume a large-scale system modeled by the following nonlinear difference equation:

$$\begin{aligned} x(k+1) &= f(x(k),u(k)) + g(x(k),w(k)) \\ y(k) &= h(x(k)) + v(k) \end{aligned} \tag{2.1}$$

where some constraints are imposed over the state variables, disturbances, and measurement noise as follows:

$$x \in \mathbb{X}, \quad w \in \mathbb{W}, \quad \text{and } v \in \mathbb{V} \tag{2.2}$$

where $x(k)$ and $y(k)$ are the state and output at k sample, $w(k)$ is the disturbance or model uncertainty, $v(k)$ is the measurement noise, and $\mathbb{X}$, $\mathbb{W}$, $\mathbb{V}$ are the feasible sets of the states, disturbances, and measurement noise, respectively. Also, $f : \mathbb{R}^n \to \mathbb{R}^n$, $g : \mathbb{R}^n \times \mathbb{R}^m \to \mathbb{R}^n$ with $g(\cdot,0) = 0$, and $h : \mathbb{R}^n \to \mathbb{R}^p$. Finally, it is assumed that $\mathbb{X}$ and $\mathbb{W}$ are closed with $0 \in \mathbb{W}$.

A linear large-scale constrained system generating the measurement sequence $\{y(k)\}$ can be derived from a linearization around each operating point of (2.1) as:

$$\begin{aligned} \hat{x}(k+1) &= A(k)\hat{x}(k) + B(k)u(k) + G(k)w(k) \\ \hat{y}(k) &= C(k)\hat{x}(k) + v(k) \end{aligned} \tag{2.3}$$

where for simplicity $\hat{x}(k) \in \mathbb{R}^n$ and $w(k) \in \mathbb{R}^w$ are the linearized state and uncertainty respectively, $v(k) \in \mathbb{R}^p$ is the linearized measurement noise, and $u(k) \in \mathbb{R}^m$ denotes the system input. Moreover, those variables are constrained as shown in (2.2). Thus, the estimation of the whole state in (2.3) can be formulated as an MHE problem as follows:

$$\Phi_k^* = \min_{x_0, \{w_j\}_{j=0}^{k-1}} \Phi_k(x_0, \{w_j\}_{j=0}^{k-1}) \tag{2.4}$$

with x_0 being the initial state. The problem is subject to the following constraints:

$$x_j \in \mathbb{X} \text{ for } j = 0, \ldots, k,\ w_j \in \mathbb{W} \text{ for } j = 0, \ldots, k-1,$$

and the cost function is:

$$\Phi_k(x_0, \{w_j\}_{j=0}^{k-1}) \triangleq \sum_{j=0}^{k-1} \|y(j) - \hat{y}(j)\|_Q^2 + \|w(j)\|_R^2 \tag{2.5}$$

The problem (2.4) gets more information as time goes and the optimization becomes intractable because the computational complexity increases at least as a linear function of time, making difficult its treatment on-line. In order to avoid this problem, a fixed dimension optimal problem by a moving horizon approximation was proposed in [1, 8, 35, 37]. With this approach, the cost function (2.5) can be written as

$$\Phi_T(x_{T-N}, \{w_k\}_{k=T-N}^{T-1}) = \sum_{k=T-N}^{T-1} \|y(k) - \hat{y}(k)\|_Q^2 + \|w(k)\|_R^2 \tag{2.6}$$

where N is the horizon of the MHE. Considering (2.6) as a cost function in the original MHE problem, the complexity of the MHE increases at least as a linear function of time until the horizon N is reached. When the horizon N is reached the complexity of the MHE problem remains constant.

2.2.2 Delay compensation using Moving Horizon Estimation

In Subsection 2.2.1, the MHE problem was introduced. In this subsection it was assumed that the measurements of the states arrive once they were taken. However, in real applications where communication networks are used to transmit the data measurements there are always delays associated transportation of the information. This may affect the performance of the estimator. Figure 2.1 shows a block diagram considering the delay on the transmission of the measurements of the states.

If there exists a delay $d(k)$ on the measurement of the states the estimation is made based on (2.3), which does not represent the dynamic behavior of the system (2.1), especially if the delay varies randomly because it is possible that future measurements of the states arrive before previous measurements. Then, the estimator may not be able to find the real value of the states, decreasing the performance of the pair MHE-controller, and thus decreasing the performance of the entire system.

Therefore, it is necessary to make a correction at the traditional MHE scheme in order to assure that the estimator calculates the appropriate value of the states. With this purpose, a variant of the MHE presented in Subsection 2.2.1 is proposed. It uses a time variant weighting matrix Q, to compute the term $\|y(k) - \hat{y}(k)\|_Q^2$ in (2.6).

Consider the system shown in Figure 2.1. Let $\widetilde{y}(k)$ denote the sequence of available measurements at time step k. Let $\widetilde{d}(k)$ denote the sequence containing the delay associated with each measurement in $\widetilde{y}(k)$. The sequence $\widetilde{y}(k)$ may not contain all the measurements on the window of the MHE because some data have not yet arrived due the delay, or may not arrive at all.

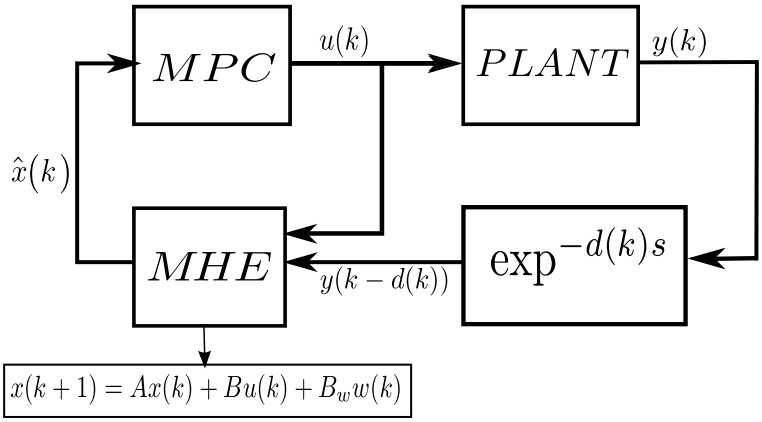

Figure 2.1: Block diagram of a control system considering the delay on the transmission of the measurements of the states.

Assume that the delay of each measurement belonging to $\widetilde{y}(k)$ is known (this is possible by using time stamps identifying the sending time of each measurement). Also, assume the delays are randomly distributed, and the delay is $d(k) = n \times T_s$ with $n \in \mathbb{N}$, being T_s the sampling time. Then, the real position of each measurement in $\widetilde{y}(k)$ can be identified and sorted accordingly to the time stamps. Also, with the sequence of delays it is possible to identify which blocks of the weighting matrix Q should be set neglected, since there is not data available to compare the estimated and the measured value. With this approach the MHE problem becomes a variable structure problem, in which the length of the sequence of available measurements and the dimension of the weighting matrix Q changes at each time step k accordingly with the available measurements.

So, the expression for computing the estimated output $\overline{y}(k)$ becomes

$$\overline{y}(k) = \begin{bmatrix} \Gamma^{N-d_1} \\ \vdots \\ \Gamma^{N-d_n} \end{bmatrix} x(k-N) + \begin{bmatrix} \Xi^{N-d_1} \\ \vdots \\ \Xi^{N-d_n} \end{bmatrix} \widetilde{u}(k) \tag{2.7}$$

where $\{d_1,\ldots,d_n\}$ is the sequence of the delays, $\Gamma^i = CA^i$, $\Xi^i = [CA^{i-1}B,\ldots,CB]$, $\widetilde{u}(k) = [u^T(k-N),\ldots,u^T(k-1)]^T$. Hence the cost function (2.6) becomes:

$$\Phi_T(x_{T-N},\{w_k\}_{k=T-N}^{T-1}) = \sum_{k=T-N}^{T-1} \|\tilde{y}(k) - \overline{y}(k)\|_Q^2 + \|w(k)\|_R^2 \tag{2.8}$$

In order to implement the proposed MHE, the following steps are suggested:

1. Given the sequence of measurements $\{y(k-N),\ldots,y(k-1)\}$, and the sequence of delays $\{d(k-N),\ldots,d(k-1)\}$, arrange the vector of measurements, where each measurement position is given by $\frac{d(k-l)}{T_s}$.
2. With the arranged vector of measurements, identify which block of the matrix Q should be neglected.
3. Estimate the states according to the MHE (see section 2.2.1).

4. After computing the estimated value of the states, send them to the controller and go back to step 1□

The following section presents some simulation results in order to compare the performance of the proposed method.

2.3 Simulation results

In this section we compared the performance of the pair MHE-MPC on a four-tank process with and without considering the proposed variable structure in the MHE, using a random normally distributed delay on the measurements. First, we performed a simulation without delay in order to set a reference behavior. Then, we added a random delay on the states measurements to show the loss of performance of the system when a fixed MHE structure is used. Finally, the proposed MHE with variable structure was implemented on the same random delay conditions to allow a comparison with the fixed structure MHE. A time-variant reference value of the controllable variables was used in order to determine the performance of the pair MHE-MPC on each of the three cases.

2.3.1 System description: the four plant process

The four-tank plant is designed to test control techniques using industrial instrumentation and control systems. The plant consists of a hydraulic process of four interconnected tanks inspired by the educational quadruple-tank process proposed by [16]. A schematic diagram of the process is shown in figure 2.2.

The target in the system showed in figure 2.2 is to regulate the level of the tanks 1 and 2, by modifying the flows q_a and q_b feeding the tanks. In this case we considered as manipulated variables the flows q_a and q_b, as controlled variables the levels h_1 and h_2, and as estimated variables the levels h_3 and h_4.

From the mass balance and the Bernoulli flow equation, the following model is proposed:

$$\begin{aligned}
\frac{dh_1}{dt} &= -\frac{a_1}{A_1}\sqrt{2gh_1} + \frac{a_3}{A_1}\sqrt{2gh_3} + \frac{\gamma_1 q_\mathrm{a}}{A_1} \\
\frac{dh_2}{dt} &= -\frac{a_2}{A_2}\sqrt{2gh_2} + \frac{a_4}{A_2}\sqrt{2gh_4} + \frac{\gamma_2 q_\mathrm{b}}{A_2} \\
\frac{dh_3}{dt} &= -\frac{a_3}{A_3}\sqrt{2gh_3} + \frac{(1-\gamma_2) q_\mathrm{b}}{A_3} \\
\frac{dh_4}{dt} &= -\frac{a_4}{A_4}\sqrt{2gh_4} + \frac{(1-\gamma_1) q_\mathrm{a}}{A_4}
\end{aligned} \tag{2.9}$$

where A_i is the cross-section area, a_i is the cross-section area of the outlet, and h_i is the level of the tank i, $i = 1,\ldots,4$. The parameters $\gamma_1,\ \gamma_2 \in [0\ 1]$ are set prior to the experiment. The flow to tank 1 is $\gamma_1 q_\mathrm{a}$ and the flow to tank 4 is $(1-\gamma_1)q_\mathrm{a}$ (and in a similar way for tanks 2 and 3). The acceleration of gravity is denoted by g. For the control test presented in this work, the plant parameters are shown in Table 2.1.

Linearizing the model at an operating point given by the equilibrium levels and flows shown in Table 2.1, and defining the deviation variables $x_i = h_i - h_{i0},\ u_j = q_j - q_{j0},\ i \in \{1,2,3,4\},\ j \in \{a,b\}$,

Table 2.1: Parameters used for the simulation of the four-tank system

Parameter	Units	Value
$h_{1\max}$	[m]	1.36
$h_{2\max}$	[m]	1.36
$h_{3\max}$	[m]	1.30
$h_{4\max}$	[m]	1.30
$h_{1\min}$	[m]	0.20
$h_{2\min}$	[m]	0.20
$h_{3\min}$	[m]	0.20
$h_{4\min}$	[m]	0.20
q_{amax}	[m^3/h]	3.26
q_{bmax}	[m^3/h]	4.00
q_{amin}	[m^3/h]	0.00
q_{bmin}	[m^3/h]	0.00
a_1	[m^2]	$1.310 * 10^{-4}$
a_2	[m^2]	$1.507 * 10^{-4}$
a_3	[m^2]	$9.267 * 10^{-5}$
a_4	[m^2]	$8.816 * 10^{-5}$
A_1	[m^2]	0.06
A_2	[m^2]	0.06
A_3	[m^2]	0.06
A_4	[m^2]	0.06
γ_1		0.3
γ_2		0.4
q_{a0}	[m^3/h]	1.63
q_{b0}	[m^3/h]	2.00
h_{10}	[m]	0.6487
h_{20}	[m]	0.6639
h_{30}	[m]	0.6498
h_{40}	[m]	0.6592

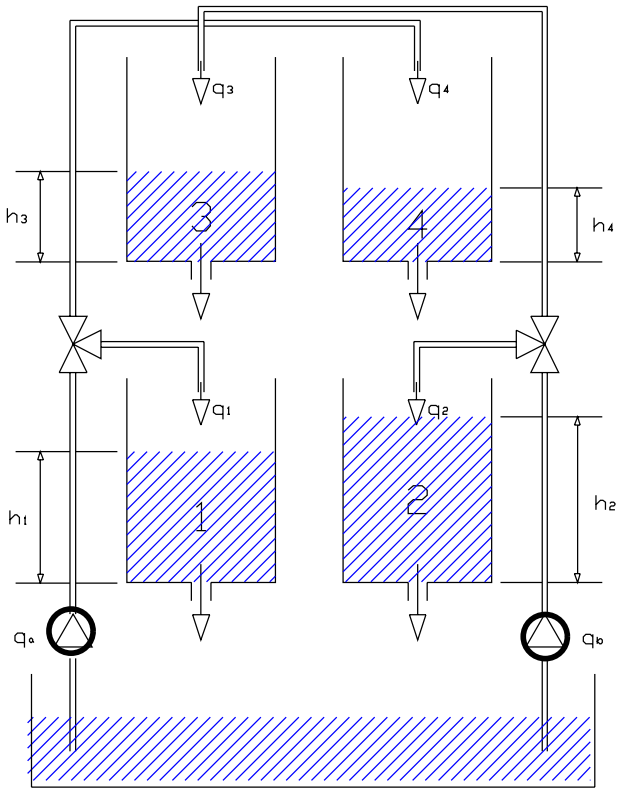

Figure 2.2: Four-tank process

the continuous-time linear model is:

$$\frac{dx(t)}{dt} = \begin{bmatrix} \frac{-1}{\tau_1} & 0 & \frac{A_3}{A_1\tau_3} & 0 \\ 0 & \frac{-1}{\tau_2} & 0 & \frac{A_4}{A_2\tau_4} \\ 0 & 0 & \frac{-1}{\tau_3} & 0 \\ 0 & 0 & 0 & \frac{-1}{\tau_4} \end{bmatrix} x(t) + \begin{bmatrix} \frac{\gamma_1}{A_1} & 0 \\ 0 & \frac{\gamma_1}{A_2} \\ 0 & \frac{(1-\gamma_2)}{A_3} \\ \frac{(1-\gamma_1)}{A_4} & 0 \end{bmatrix} u(t) \tag{2.10}$$

$$y(t) = \begin{bmatrix} 1 & 0 & 0 & 0 \\ 0 & 1 & 0 & 0 \end{bmatrix}$$

where $\tau_i = \frac{A_i}{a_i}\sqrt{\frac{2h_{i0}}{g}} \geq 0,\ i \in \{1,2,3,4\}$ are the time constants of tank i. For the parameters chosen the linear system shows four real stable poles and two non-minimum phase multivariable zeros.

With the purpose of applying the proposed MHE, the model (2.10) was discretized with a sample time $T_s = 5$ s. The resulting model also was used as a prediction model in the MPC.

2.3.2 Simulation Results

In order to test the proposed MHE, three cases were considered:

1. The measurements of the states were taken without delay.
2. The measurements of the states were taken with delay and a fixed structure MHE was implemented.

3. The measurements of the states were taken with delay and the proposed MHE was implemented.

In these three cases the reference signal shown in figure 2.3 was considered. The horizon for the MHE was 200 sample times, and the prediction horizon for the MPC was 90 sample times. For the cases 2 and 3, the delay was considered normal distributed with mean $\mu = 12$ and variance $\sigma^2 = 12$ times the sample time.

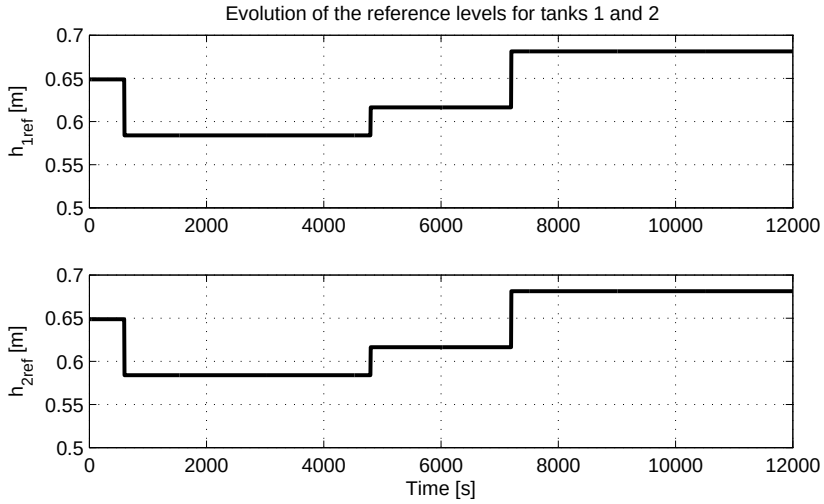

Figure 2.3: Reference signal. Top, the reference for the level of the tank 1, and bottom, the reference signal for the level of the tank 2.

Figures 2.4 and 2.5 show the behavior of the system (2.9) when there was no delay in the measurement of the states. From Figure 2.4 it is possible to conclude that the values of the states given by the MHE converge to their real values. Figure 2.5 shows that the pair MHE-MPC is able to lead the controllable variables of the system to their desired values, despite of the changes on the set-point.

In Figure 2.4, note that after the convergence of the MHE (and despite of the changes on the reference values of the controllable variables) the values of the states estimated by the MHE are the same than their real values. But, if a time delay is included in the measurements of the states, the performance of the system decreases, as shown on Figures 2.6 and 2.7.

Figures 2.6 and 2.7 show that despite of the convergence of the MHE, the pair MHE-MPC is not able to lead the controllable variables to their set-point, and that the delay induce an oscillatory behavior in (2.9).

In order to avoid the effects of the delay on the system (2.9) (which are displayed on Figures 2.6 and 2.7), the proposed MHE was implemented for the four-tank system. Figures 2.8 and 2.9 show the behavior of the system when the random delay is considered and the proposed MHE is implemented. Figure 2.8 shows that the value of the estimates reached the real values without oscillations despite of the random delay and the changes on the set-points of the controllable variables. Figure 2.9 presents the entire system behavior. In comparison with the behavior of the system without delay (Figure 2.3), with the initial set-point it is observed an expected delay on the convergence of the controllable variables to their reference values, due to the lack of available data for the state estimation. On the following set-point changes their behavior is quite similar, i.e., the proposed variable structure MHE neglected the random delay conditions. However, the control actions computed by the MPC under

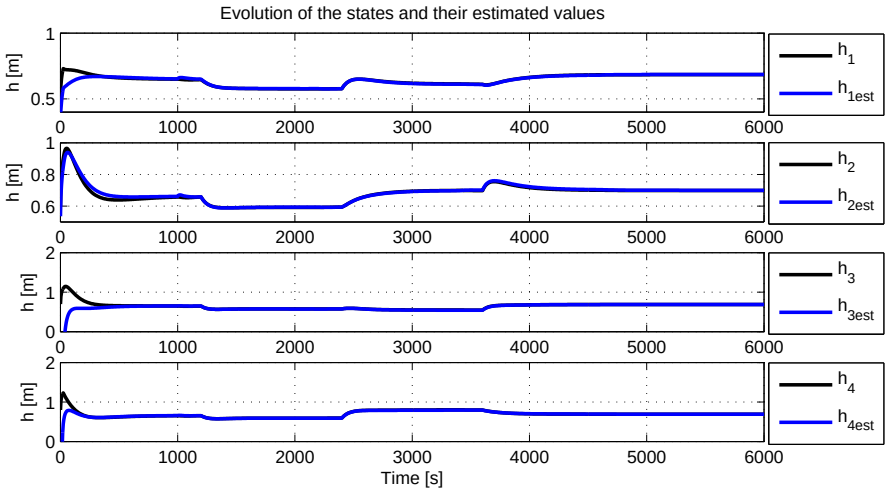

Figure 2.4: Evolution of the real and estimated levels.

random delay conditions and with the proposed variable structure MHE, were larger in amplitude compared with the control actions without delay and fixed structure MHE.

2.4 Conclusions

In this work the problem of the random delay in the measurements of the states was considered. Here, the delay was assumed random, known, and n times the sample time ($n \in \mathbb{N}$). In order to handle this problem a variable structure MHE was proposed, where the delayed measurements of the states were arranged in a vector of measurements containing the real positions of the arriving values of the states.

As test bed, the four-tank system was used. A pair MHE-MPC was implemented in order to control it, with two MHE structures: fixed and variable. Variations on the reference value of the controlled variables were made with the purpose of testing the performance of the pair MHE-MPC. When a random delay was included into the measurements of the states, the pair MHE-MPC with fixed MHE structure fell into an oscillatory behavior. Under the same conditions, the proposed MHE improved the performance of the pair MHE-MPC, exhibiting a performance similar than the pair MHE-MPC without delay. Then, it is possible to conclude that the MHE with variable structure proposed on this work neglects the effect of the random delay on the measurements.

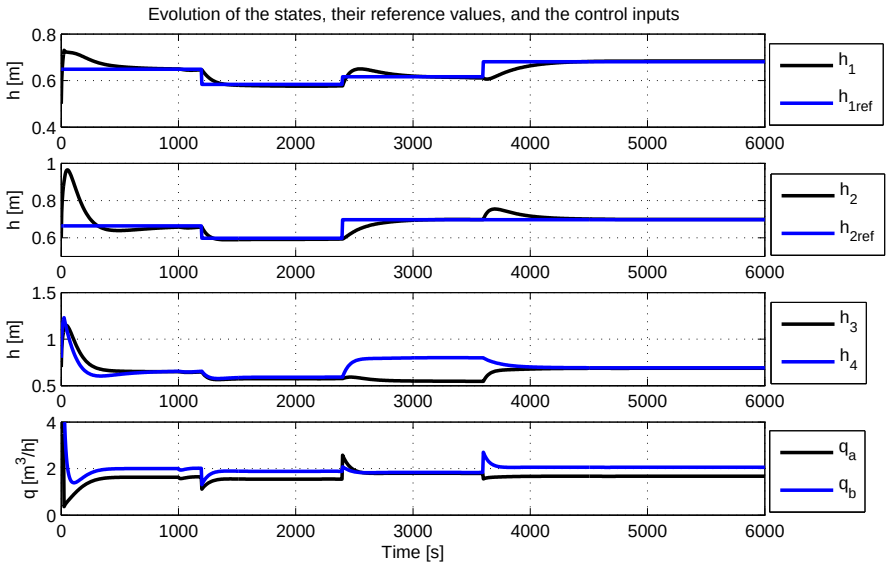

Figure 2.5: Evolution of the levels h_1 and h_2, and their reference values (first two panels), of the levels h_3 and h_4 (third panel), and of the control inputs q_a and q_b.

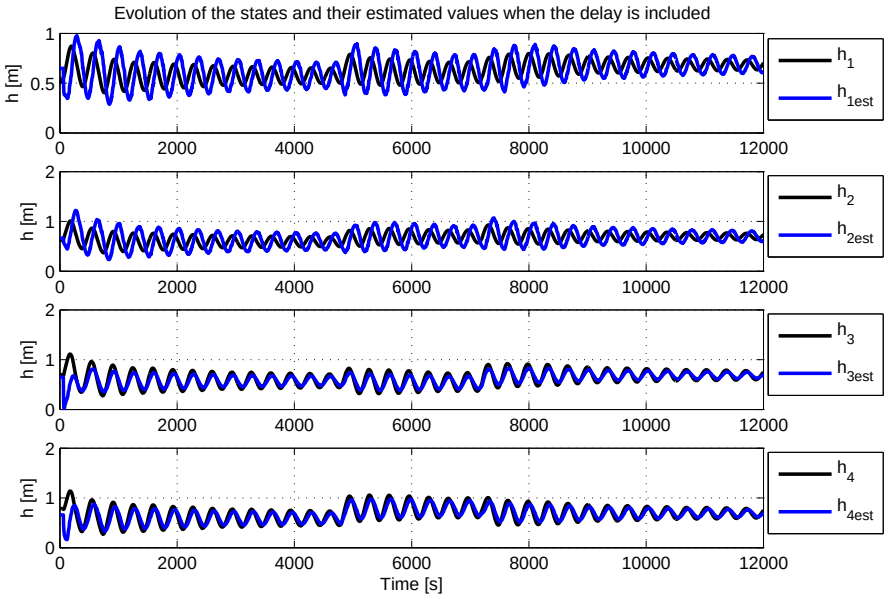

Figure 2.6: Evolution of the real and estimated levels when the delay is included.

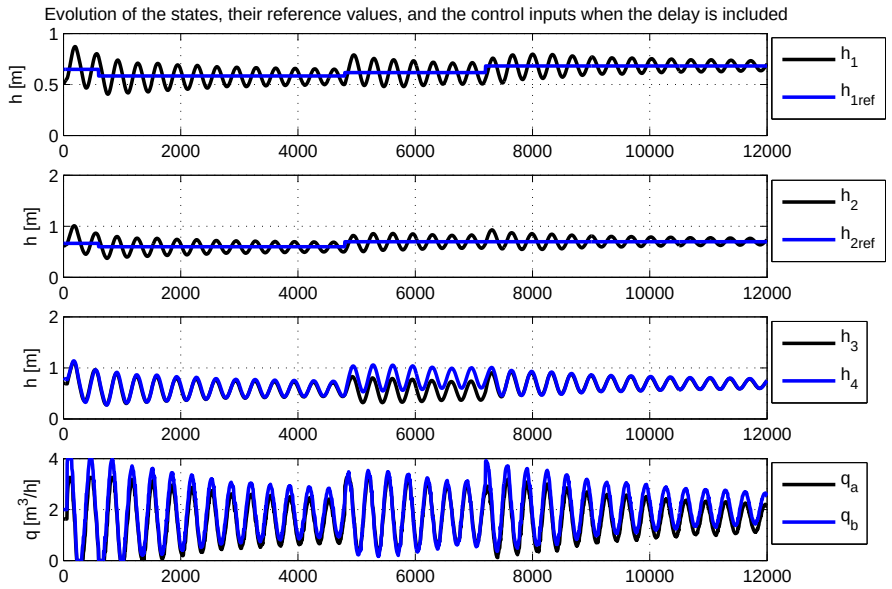

Figure 2.7: Evolution of the levels h_1 and h_2, and their reference values (first two panels), of the levels h_3 and h_4 (third panel), and of the control inputs q_a and q_b, when the delay is included.

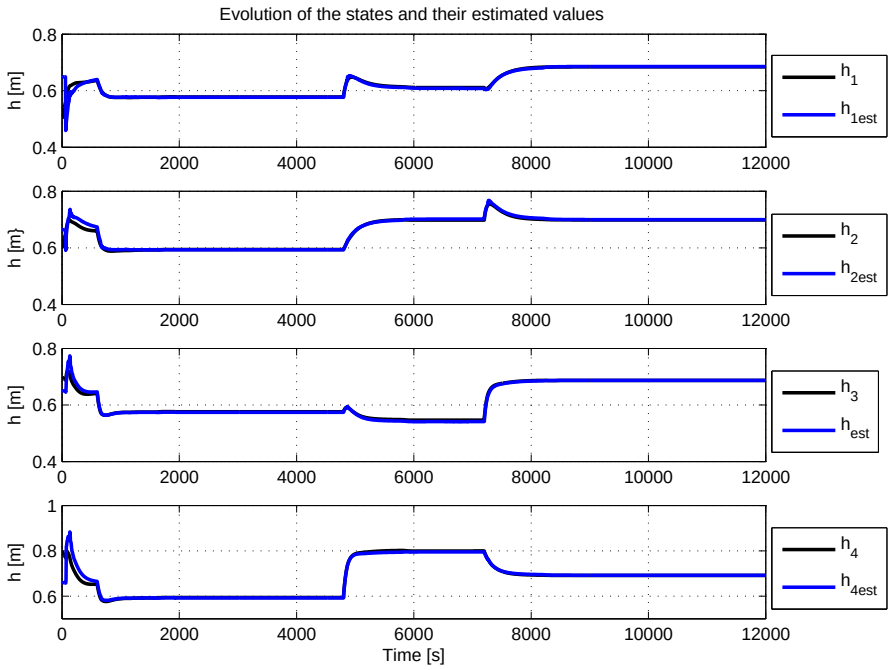

Figure 2.8: Evolution of the real and estimated levels when the proposed MHE is implemented.

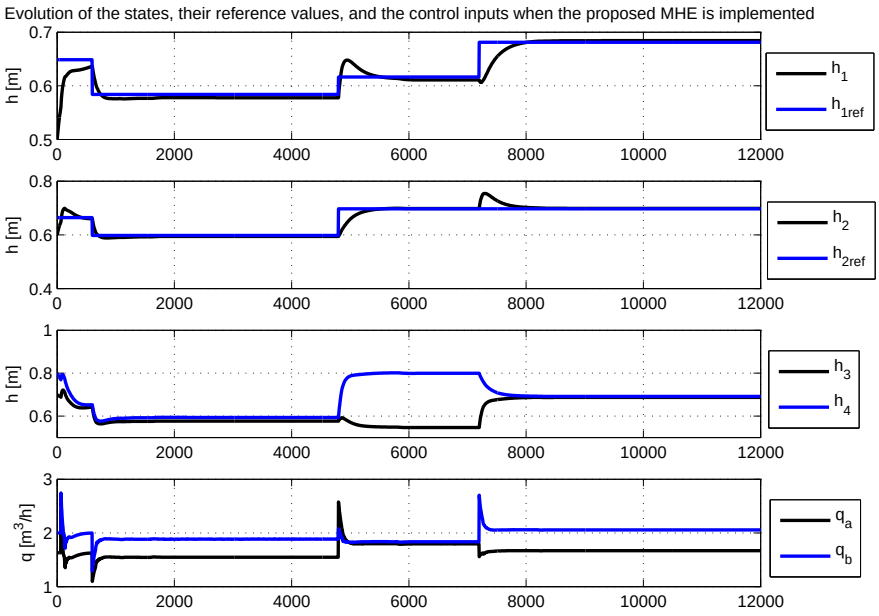

Figure 2.9: Evolution of the levels h_1 and h_2, and their reference values (first two panels), of the levels h_3 and h_4 (third panel), and of the control inputs q_a and q_b, when the proposed MHE is implemented.

Chapter 3

On the Explicit Dead-Time Compensation in Robust MPC. Application to a Laboratory Heater Process

3.1 Introduction

Intrinsic dead-time compensation is one of the advantages of model predictive control (MPC) [5]. However, stability of the MPC schemes is related to a terminal cost, a terminal set, and a stabilizing control law [26] which are usually derived from a delay free model. In theory, this problem can be systematically solved by using an augmented representation [2] but, in this approach, the representation order increases linearly with the dead-time length. This dependence is not interesting in practice because the order of the model may affect the computational burden especially in robust MPC strategies.

Dead-time compensation schemes have been known in the control community since Smith's seminal work [41]. In general, dead times are not considered to be a problem for MPC strategies due to the intrinsic compensation property. Actually, an explicit compensation strategy can be useful in two situations: i) in order to avoid the augmented representation as used in [36], or ii) in order to improve robustness as discussed in [30].

An explicit compensation scheme was briefly explored in [36] in order to reduce the representation order but its effect on robustness was not analyzed. In [31], a filtered Smith predictor scheme was used to improve robustness of the generalized predictive controller (GPC) but, analytical discussions were limited to the unconstrained case. The problem of robustness in the presence of dead-time uncertainty was treated in [32] by using a polytopic approach. However, in that case, it was necessary to consider an augmented state representation for delays that are larger than a sampling period. It is important to emphasize that in none of these works, robust constraint satisfaction and standard state representation are considered together.

In this chapter, following the ideas of [38, 39], a robust explicit dead-time compensation for constrained linear systems with additive disturbances will be presented. It will be shown that the dead-time free prediction model can be used to guarantee robust stability and robust constraint satisfaction by using a modified disturbance and a slightly different state constraint set. The effect of this modified disturbance will be discussed in terms of input-to-state stability and robust constraint satisfaction.

Additionally, a robust MPC for tracking will be particularized for first-order (or integrative) plus dead-time models (FOPDT/IPDT)[1] [39] in order to take some advantages of the proposed compensation scheme, deriving a simple explicit robust control law. A simulation examples and an experimental case of study will be presented to discuss about the properties of the proposed algorithm.

The chapter is organized as follows: delay compensation background is presented in Section 3.2, an analysis of the additive disturbance effect is presented in Section 3.3, and a tube based MPC is revisited to be used in time delay systems in Section 3.4. In Section 3.5 an experimental case study is presented, while the concluding remarks are discussed in Section 3.6.

Notation: A definite positive matrix T is denoted as $T > 0$. For a given symmetric matrix $P > 0$, the weighted Euclidean norm is expressed as $||x||_P = \sqrt{x'Px}$. A vector concatenation is represented by $(a,b) = [a',b']'$. Given two sets $\mathbb{U} \subset \mathbb{R}^n$ and $\mathbb{V} \subset \mathbb{R}^n$, the Minkowski sum is defined by $\mathbb{U} \oplus \mathbb{V} \triangleq \{u+v \mid u \in \mathbb{U},\ v \in \mathbb{V}\}$ and the Pontryagin set difference is $\mathbb{U} \ominus \mathbb{V} \triangleq \{u \mid u \oplus \mathbb{V} \subseteq \mathbb{U}\}$. The distance of a point $u \in \mathbb{R}^n$ from a set $\mathscr{V} \subseteq \mathbb{R}^n$ is denoted by $\sigma(u,\mathscr{V}) \triangleq \inf_v\{||u-v|| \mid v \in \mathscr{V}\}$, where $||.||$ denotes the Euclidean norm. For a given matrix $M \in \mathbb{R}^{n\times m}$ and a set $\mathbb{V} \subset \mathbb{R}^m$, $M\mathbb{V} \subset \mathbb{R}^n$ denotes the set $\{y = Mv,\ v \in \mathbb{V}\}$. A identity matrix is represented by I. Predictions for the time i computed at k will be represented by $u(i|k)$, $x(i|k)$ and $y(i|k)$.

3.2 Preliminaries

In this section, some ideas of dead-time compensation MPC will be briefly revisited in terms of a state-space model with dead-time [39].

3.2.1 Implicit dead-time compensation

In MPC formulations, stability is related to three elements: a terminal cost, a terminal constraint and a local stabilizing control law [26]. For linear models without delay such as

$$x(k+1) = Ax(k) + Bu(k),\ \ y(k) = Cx(k),$$

MPC stabilizing control law is obtained from the current state $u(k) = \kappa_{MPC}(x(k))$.

However, in systems with dead-time such as

$$x(k+1) = Ax(k) + Bu(k-d),\ \ y(k) = Cx(k), \tag{3.1}$$

$x(k+1)$ is not defined by the pair $x(k)$, $u(k)$. As consequence, Eq. (3.1) cannot be directly used in a MPC strategy because $x(k)$ is not enough not represent the overall dead-time system dynamic. Fortunately, an augmented model can be used as in [2], incorporating the dead-time effect as a dead-beat dynamic, in order to obtain a "dead-time free" representation given by

$$\xi(k+1) = A_\xi \xi(k) + B_\xi u(k),\ \ y(k) = C_\xi \xi(k) \tag{3.2}$$

with

$$\xi(k) = [x(k)'\ u(k-d)'\ \ldots\ u(k-2)'\ u(k-1)'],$$

[1] For the sake of simplicity, the term FOPDT will be used to refer to stable, unstable, or integrative processes with dead-time from now on.

$$A_\xi = \begin{bmatrix} A & B & 0 & 0 & ... & 0 \\ 0 & 0 & I & 0 & ... & 0 \\ \vdots & \vdots & \vdots & \vdots & \ddots & \vdots \\ 0 & 0 & 0 & 0 & ... & I \\ 0 & 0 & 0 & 0 & ... & 0 \end{bmatrix}, B_\xi = \begin{bmatrix} 0 \\ 0 \\ \vdots \\ 0 \\ I \end{bmatrix}, C'_\xi = \begin{bmatrix} C' \\ 0 \\ \vdots \\ 0 \\ 0 \end{bmatrix}.$$

The underlying idea is to store the past control actions in $\xi(k)$ until the moment it can actually be considered. In this case, $\xi(k+1)$ depends only on $\xi(k)$ and $u(k)$ in order that stabilizing elements can be directly defined.

3.2.2 Explicit dead-time compensation

A simple idea, discussed in [36], can be applied to consider a prediction model without dead-time. From the model (3.1), it can be observed that there is no effect of $u(k)$ over $x(k+1|k)$, $x(k+2|k)$, ..., $x(k+d|k)$ due to the dead-time. As consequence, $x(k+d|k)$ depends only on past controls so that it can be obtained recursively from Eq. (3.1) by using

$$x(k+d|k) = A^d x(k) + \sum_{j=1}^{d} \left[A^{j-1} B u(k-j)\right]. \tag{3.3}$$

Hence, it would be reasonable to control directly $x(k+d+1|k)$ because $x(k+d|k)$ is already determined and explicitly calculated. In this case, the new controlled state can be defined as

$$\tilde{x}(k) \triangleq x(k+d|k) \tag{3.4}$$

where $x(k+d|k)$ can be obtained from Eq. (3.3). As a consequence, the system to be controlled becomes

$$\tilde{x}(k+1) = A\tilde{x}(k) + Bu(k), \;\; y(k+d|k) = C\tilde{x}(k) \tag{3.5}$$

which has a dead-time free model. The key point is that due to the compensator structure, the model (3.5) can be directly used in MPC strategies without resort to an augmented representation as presented in Eq. (3.2).

An overall control structure is depicted Fig. 3.1 where $w(k)$ is a general disturbance which may be used to represent unmeasured inputs, noise and process-model mismatch. Similarly to other dead-time compensators [30], an MPC is used to control a dead-time free system which may be represented by the "process with dead-time plus a predictor" where nominal model is given by Eq. (3.5). This prediction scheme is exact in the nominal case because $x(k+d|k) = x(k+d)$. However, in the presence of disturbance, $x(k+d|k) \neq x(k+d)$ which should be considered in robust MPC strategies.

3.3 Main results

Now, the explicit compensation effect will be analyzed in terms of a state additive disturbance in order to consider robust stability and constraint satisfaction. Hence, the real dynamic is represented by

$$x(k+1) = Ax(k) + Bu(k-d) + w(k). \tag{3.6}$$

with $w(k) \in \mathbb{W}$ where $\mathbb{W}$ is a compact polytope which contains the origin. It is important to emphasize that the effect of noise, external unmeasured disturbance and process-model mismatches (including

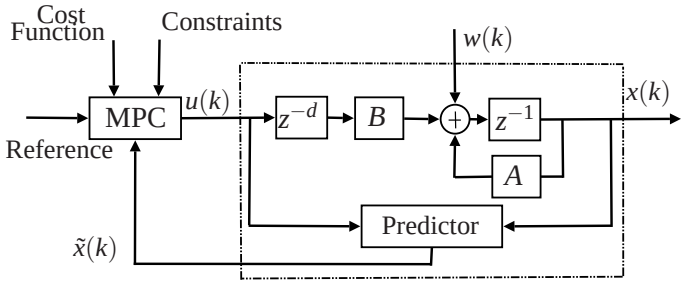

Figure 3.1: MPC with explicit delay compensation structure.

dead-time estimation uncertainty) appears in $w(k)$. By considering the explicit compensation scheme given by Eqs. (3.3) and (3.4), the predicted behavior can be described by

$$\tilde{x}(k+1) = A\tilde{x}(k) + Bu(k) + \tilde{w}(k) \tag{3.7}$$

where $\tilde{w}(k)$ is the effect of $w(k)$ on the predicted state ($\tilde{x}(k)$).

From Eq. (3.7), $\tilde{w}(k)$ can be obtained by

$$\tilde{w}(k) = \tilde{x}(k+1) - A\tilde{x}(k) - Bu(k). \tag{3.8}$$

Then, by replacing Eqs. (3.3) and (3.4) in Eq. (3.8), it is obtained

$$\begin{aligned}\tilde{w}(k) =& A^d x(k+1) + \sum_{j=1}^{d} [A^{j-1} Bu(k-j+1)] \\ & - A\left\{ A^d x(k) + \sum_{j=1}^{d} [A^{j-1} Bu(k-j)] \right\} - Bu(k) \\ =& A^d [x(k+1) - Ax(k) - Bu(k-d)].\end{aligned} \tag{3.9}$$

Finally, replacing Eq. (3.6) in Eq. (3.9) yields

$$\tilde{w}(k) = A^d w(k). \tag{3.10}$$

This result is important because for a given system, $\tilde{w}(k)$ is uniquely determined by $w(k)$ so that for $w(k) \in \mathbb{W}$, $\tilde{w}(k) \in A^d \mathbb{W} \triangleq \tilde{\mathbb{W}}$.

3.3.1 Bounding prediction error

If there are constraints on the state, it is necessary to guarantee robust constraint satisfaction of $x(k)$ instead of $\tilde{x}(k)$. Thus, prediction error should be analyzed once $\tilde{x}(k)$ is the variable used for control purposes.

The prediction error can be obtained by

$$e(k) = x(k) - x(k|k-d) = x(k) - \tilde{x}(k-d). \tag{3.11}$$

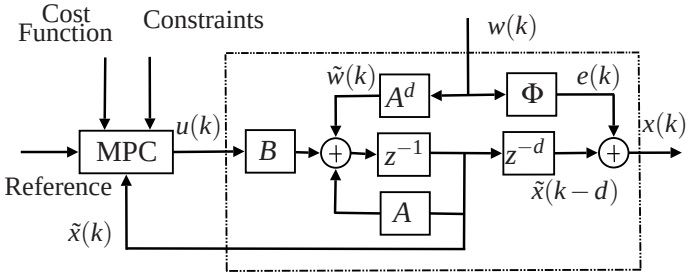

Figure 3.2: MPC with explicit delay compensation structure.

Thus, by using Eq. (3.6) recursively from $x(k-d+1)$ until $x(k)$, it is possible to rewrite $x(k)$ as

$$\begin{aligned} x(k) =& A^d x(k-d) + \sum_{j=1}^{d} \left[A^{j-1} B u(k-j-d)\right] \\ &+ \sum_{j=1}^{d} \left[A^{j-1} w(k-j)\right] \end{aligned} \tag{3.12}$$

Moreover, $\tilde{x}(k-d)$ is obtained from $x(k|k-d)$ in Eq. (3.3):

$$\tilde{x}(k-d) = A^d x(k-d) + \sum_{j=1}^{d} \left[A^{j-1} B u(k-j-d)\right]. \tag{3.13}$$

Then, by replacing Eq. (3.13) and Eq. (3.12) at Eq. (3.11), it is obtained the following prediction error expression

$$e(k) = A^{d-1} w(k-d) + A^{d-2} w(k-d+1) + \ldots + w(k-1). \tag{3.14}$$

It should be noticed that disturbance has a cumulative effect in the prediction error but, if $w(k)$ is bounded, $e(k)$ is also bounded. Finally, the prediction error may be bounded by

$$\mathbb{E} = A^{d-1}\mathbb{W} \oplus A^{d-2}\mathbb{W} \ldots \oplus \mathbb{W}. \tag{3.15}$$

Similarly to [25], once the error is bounded, it can be concluded that if

$$\tilde{x}(k) \in \mathbb{X} \ominus \mathbb{E},\ \forall k \geq 0 \Rightarrow x(k) \in \mathbb{X},\ \forall k \geq d.$$

Note that $\mathbb{E}$ is also a compact polytope which contains the origin.

The schematic representation of the explicit optimal prediction in the presence of additive disturbance is shown in Fig. 3.2 where

$$\Phi = \sum_{j=1}^{d} A^{j-1} z^{-j}.$$

This representation is equivalent to those of Fig. 3.1 when $\tilde{x}(k)$ is computed as in Eqs. (3.3) and (3.4). Despite the fact that it is considered $\tilde{x}(k)$ for control purposes, the effect of $w(k+j)$ for $j > 0$ does not affect the loop so that robust stability is associated with $\tilde{w}(k)$ and, as consequence, it does not depends on $w(k+1)$,...,$w(k+d)$ at k.

3.3.2 Analysis of robustness and constraint satisfaction

Now, the explicit compensation effect will be considered in the context of a general control law $\kappa(\cdot)$ formulated in terms of the following Lemma.

Lemma. 2

(i) *Let $u(k) = \kappa(\tilde{x}(k))$ be a control law such that*

$$\tilde{x}(k+1) = A\tilde{x}(k) + Bu(k) + \tilde{w}(k)$$

is input-to-state stable (ISS) with $\tilde{w}(k) \in A^d\mathbb{W}$ and F_∞ be its minimum robust positively invariant set.

(ii) *Let*

$$x(k+1) = Ax(k) + B\kappa(\tilde{x}(k-d)) + w(k)$$

be a system with $w(k) \in \mathbb{W}$, $\mathbb{E} = \bigoplus_{j=1}^{d} A^{j-1}\mathbb{W}$ and

$$\tilde{x}(k-d) = A^d x(k-d) + \sum_{j=1}^{d} \left[A^{j-1}Bu(k-j-d)\right].$$

Then:

(a) *System (ii) is input-to-state stable for $\forall w(k) \in \mathbb{W}$ and $\sigma(x(k), F_\infty \oplus \mathbb{E}) \to 0$. Moreover, if $w(k) \to 0$, $x(k) \to 0$;*

(b) *If $\tilde{x} \in \mathbb{X} \ominus \mathbb{E}$, $\forall k \geq 0$, then $x(k) \in \mathbb{X}$, $\forall k \geq d$.*

Qualitatively, Lemma 2 means that, for a given control law, if a system without dead-time is ISS with $\tilde{w}(k) \in A^d\mathbb{W}$, a similar system with $w(k) \in \mathbb{W}$ and that have dead-time d is ISS if the given control law is applied together with the explicit dead-time compensation scheme. Moreover, if it is possible to guarantee that the system without dead-time is constrained to $\tilde{x}(k) \in \mathbb{X} \ominus \mathbb{E},\ k \geq 0$ then, the real state is such that $x(k) \in \mathbb{X},\ k \geq d$. This result is somehow general because the law $u(k) = \kappa(\tilde{x}(k))$ is not defined. As a consequence, robust MPC schemes are natural candidates to guarantee the conditions of Lemma 2.

This Lemma also allows to derive a different interpretation of the predictor effect. The following illustrative discussion will be presented to show that this result can be somehow counterintuitive.

3.4 Robust tube based MPC with explicit dead-time compensation

In order to ensure that conditions (i) and (ii) of Lemma 2 holds, it is possible to use the so different strategies such as in [7] and [27]. In this chapter, we consider the tracking problem [22] instead of the regulation one [27]. This is motivated due to the fact that it is more useful in practice and in the presence of constant disturbance, an additional reference correction should be considered [39].

Consider the following uncertain system

$$x^+ = Ax + Bu + w, \quad y = Cx \tag{3.16}$$

where $x \in \mathbb{R}^n$ is the current state, x^+ is the successor state, $u \in \mathbb{R}^m$ is the current control $w \in \mathbb{R}^n$ is an unknown disturbance and $y \in \mathbb{R}^p$ is a desired linear combination of the states. In this case: $x = \tilde{x}(k)$, $x^+ = \tilde{x}(k+1)$ $w = \tilde{w}(k)$, and $y = y(k+d|k)$ subject to compact and convex polyhedral constraints

$$x \in \mathbb{X} \ominus \mathbb{E} \subset \mathbb{R}^n, \quad u \in \mathbb{U} \subset \mathbb{R}^m \tag{3.17}$$

and a disturbance constraint

$$w \in \tilde{\mathbb{W}} \subset \mathbb{R}^n.$$

As proposed in [22], the overall objective is to stabilize the constrained system and steer the state to a neighborhood of the set-point fulfilling the constraints for any possible disturbance.

3.4.1 Tubes trajectory

This robust MPC strategy is based on the notion of tubes and robust positive invariance. Some of these ideas are briefly revisited in the following. From now on, the nominal behavior will be compactly described by

$$\bar{x}^+ = A\bar{x} + B\bar{u} \quad \bar{y} = C\bar{x}. \tag{3.18}$$

A feedback control law can be used to counteract the disturbance effect as the following

$$u = \bar{u} + K\delta, \quad \delta \triangleq x - \bar{x}$$

where δ is defined as the state error. Hence, the error dynamics is described by

$$\delta^+ = A_K\delta + w; \quad A_K = (A + BK). \tag{3.19}$$

If A_K is strictly stable[2], there exist, for system (3.19), a robust positively invariant set $\mathscr{Z}$ [18, 34] that satisfies

$$A_K\mathscr{Z} \oplus \tilde{\mathbb{W}} \subseteq \mathscr{Z}.$$

Assuming that $\delta(0) = x(0) - \bar{x}(0) \in \mathscr{Z}$, the tubes notion comes from the fact that if $\bar{u}$ is such that

$$\bar{x} \in \overline{\mathbb{X}} = \mathbb{X} \ominus \mathbb{E} \ominus \mathscr{Z}, \quad \bar{u} \in \overline{\mathbb{U}} = \mathbb{U} \ominus K\mathscr{Z}, \tag{3.20}$$

then

$$x \in \mathbb{X} \ominus \mathbb{E}, \quad u \in \mathbb{U}$$

for any sequence of $w \in \mathbb{W}$ (any disturbance realization) [27].

3.4.2 Predictive controller for reference tracking

To avoid problems such as feasibility loss due to reference change or reference inconsistency with the prediction model, an artificial stationary point is used [22].

Assumption. 1 *The pair (A, B) is stabilizable and all the states are available at each sampling time.*

[2] All the eigenvalues of A_K are strictly inside the unitary circle.

Under this assumption, the set of steady states and inputs of the system (3.18) is an m-dimensional subspace of $\mathbb{R}^{n+m}$ [22] given by the parameterization

$$(\bar{x}_s, \bar{u}_s) = M_\theta \overline{\theta}.$$

In other words, every steady-state pair $(\bar{x}_s, \bar{u}_s) \in \mathbb{R}^{m+n}$ is uniquely characterized by a given parameter $\overline{\theta} \in \mathbb{R}^m$.

In the robust tube based MPC for reference tracking, the initial nominal state ($\bar{x}(0)$), the nominal sequence of future control action ($\overline{\mathbf{u}}$) and the parameter $\overline{\theta}$, which defines $(\bar{x}_s, \bar{u}_s)$, are decision variables. The cost function is given by

$$\begin{aligned} V(x, y_r; \mathbf{u}, \bar{x}, \overline{\theta}) = \sum_{i=0}^{N-1} ||\bar{x}_i - \bar{x}_s||_Q^2 + ||\bar{u}_i - \bar{u}_s||_R^2 \\ + ||\bar{x}_N - \bar{x}_s||_P^2 + V_o(\bar{y}_s - y_r). \end{aligned}$$

where $\bar{x}_i$ denotes the prediction of $\bar{x}$ i-samples ahead, $(\bar{x}_s, \bar{u}_s) = M_\theta \overline{\theta}$ characterizes the artificial stationary point, $\bar{y}_s = C\bar{x}_s$ is an admissible artificial set-point, y_r is the desired reference for y and $V_o(\bar{y}_s - y_r)$ is an off-set cost [9]. Therefore, the following optimization problem should be solved at each sampling instant

$$\begin{aligned} \min_{\bar{x}(0), \overline{\mathbf{u}}, \overline{\theta}} \quad & V(x, y_r; \bar{x}(0), \overline{\mathbf{u}}, \overline{\theta}) \\ \text{s.t.} \quad & \\ & \bar{x}_0 \in x \oplus (-\mathscr{Z}) \\ & \bar{x}_i \in \mathbb{X} \ominus \mathbb{E} \ominus \mathscr{Z}, \quad i = 0, 1, ..., N-1 \\ & \bar{u}_i \in \mathbb{U} \ominus K\mathscr{Z}, \quad i = 0, 1, ..., N-1 \\ & (\bar{x}_N, \overline{\theta}) \in \Omega_{t,\bar{K}}. \end{aligned}$$

where Ω_{t,K_Ω} is an extended invariant set for tracking by using a given stabilizing controller K_Ω. In this case, the extended system for tracking is

$$\begin{bmatrix} \bar{x} \\ \overline{\theta} \end{bmatrix}^+ = \begin{bmatrix} A + BK_\Omega & BL \\ 0 & I \end{bmatrix} \begin{bmatrix} \bar{x} \\ \overline{\theta} \end{bmatrix}$$

where $L = [-K_\Omega \; I] M_\theta$ and the invariant region should be admissible in

$$\mathbb{X}^e = \left\{ x^e \triangleq (\bar{x}, \overline{\theta}) : (\bar{x}, K_\Omega \bar{x} + L\overline{\theta}) \in (\overline{\mathbb{X}} \times \overline{\mathbb{U}}),\ M_\theta \theta \in (\overline{\mathbb{X}} \times \overline{\mathbb{U}}) \right\}.$$

Finally, The MPC control law is

$$K_{MPC}(x, y_r) = \bar{u}^*(0; x, y_r) + K(x - \bar{x}^*(x, \overline{\theta}))$$

where $\bar{u}^*(0; x, y_r)$ is the first element of the optimal nominal control sequence ($\overline{\mathbf{u}}$) and $\bar{x}^*$ is the optimal nominal value for $x(0)$.

The following additional assumptions on the MPC parameters are sufficient to guarantee stability:

Assumption. 2

1. *Let $R > 0$ e $Q \geq 0$ such that the pair $(Q^{1/2}, A)$ is observable.*
2. *Let $P \in \mathbb{R}^{n\times n}$ be a positive definite matrix such that*

$$(A + BK_\Omega)^T P(A + BK_\Omega) - P + K_\Omega^T R K_\Omega + Q = 0.$$

3. *Let the offset cost function $V_o : \mathbb{R}^p \to \mathbb{R}$ be a convex, positive definite and sub-differentiable function such that $V_o(0) = 0$.*

For details, please refer to [22].

Remark. 1
In the proposed robust tube based controller, if $\tilde{x}(0)$ is admissible, Lemma 2 holds and robust constraint satisfaction is ensured for $x(k)$, $\forall k \geq d$. It should be noticed that $x(j)$, $j \in [1,d]$ depends on $x(0)$ and $u(i)$, $i = [-d,-1]$. Thus, if $u(i)$, $i = [-d,-1]$ is known, robust constraint satisfaction for $x(j)$, $j \in [1,d]$ can be previously verified.

3.4.3 Output offset cancellation in the presence of constant disturbance

In the presence of persistent disturbance, an undesired error will appear because the stationary point parameterization does not consider this disturbance. In this case, a modified reference $y_r^m(k)$ may defined by

$$y_r^m(k) = y_r - y_s^w(k) = y_r - M\hat{w}(k)$$

where $M \in \mathbb{R}^{p\times n}$ is a constant matrix and $\hat{w}(k)$ is an estimation of $w(k)$. If the disturbance estimator is stable and converges to $\hat{w}(k) = w(\infty)$, then $y(k)$ will converge to y_r if it is admissible. Due to separation principle, if $\hat{w}(k) \in \mathbb{W}$, this outer loop does not affect stability because constant disturbance estimation in not related with MPC control law.

An interesting property of this algorithm is that it results in a quadratic optimization problem which does not depends on the dead-time length. Similarly to [32], the optimization problem can parameterized off-line with multiple piecewise linear solutions [4]. However, by using the standard approach as in [32], the longer is the dead-time, the higher is the dimension of the state partition where the linear solution must be searched. In [11], for instance, it is presented an integrative process with 40 discrete delays which means that the state partition would have dimension 41 in the standard approach. By considering only the regulation problem, the partition of the robust tube MPC with explicit dead-time compensation would have dimension 1. In the case of reference tracking the dimension is simply 2.

3.4.4 First order plus dead-time case

The proposed robust tube based MPC will be particularized to discrete FOPDT models. This is motivated by some reasons: these kind of models are common in practice, it becomes much easier to analyze and to obtain the invariant sets, it is not necessary to consider state-estimation and the discussions about dead-time compensator effect becomes more intuitive [39]. However, it is important to

emphasize that all the ideas presented until now can be applied to linear state-space models. Furthermore, if necessary, it is possible to consider state-space estimation following the ideas of [25].

Now, consider a model given by

$$P(z) = \frac{k_p}{z-a} z^{-d}$$

and a dead-time free state-space representation (A,B,C,D) with $A=[a]$, $B=[k_p]$, $C=1$ and $D=0$. In this case, the stationary point parameterization can be defined in such a way that θ is the desired reference ($\theta = y_r$) with $M_\theta = [1\ (1-a)/k_p]'$ and $N_\theta = 1$.

The main advantage of this simplified representation is that set operations such as Minkowski sum and Pontryagin difference should be considered in sets of the space $\mathbb{R}^1$. Thus, it will be just necessary to consider standard algebraic operations in the limits of the set interval. Now, it will be considered that the feedback law is in the form $K = (b-a)/(k_p)$ in such a way that $A+BK = b$ with $0 \leq b < 1$, the constraints are $\mathbb{U} = \{u : u_{min} \leq u \leq u_{max}\}$, $\mathbb{X} = \{x : x_{min} \leq x \leq x_{max}\}$ and the disturbance is in the interval $\mathbb{W} = \{w : w_{min} \leq w \leq w_{max}\}$. In this case, the disturbance effect is given by:

$$\begin{aligned} \mathscr{Z} &= a^d\mathbb{W} \oplus ba^d\mathbb{W} \oplus b^2a^d\mathbb{W} \oplus b^3a^d\mathbb{W} \oplus ... \\ &= \left\{ \zeta : \frac{a^d}{1-b} w_{min} \leq \zeta \leq \frac{a^d}{1-b} w_{max} \right\}; \end{aligned} \tag{3.21}$$

$$\begin{aligned} \mathbb{E} &= \mathbb{W} \oplus a\mathbb{W} \oplus a^2\mathbb{W} \oplus ... \oplus a^{d-1}\mathbb{W} \\ &= \left\{ \varepsilon : \frac{(1-a^d)}{1-a} w_{min} \leq \varepsilon \leq \frac{(1-a^d)}{1-a} w_{max} \right\}. \end{aligned} \tag{3.22}$$

As it was already pointed out that, for stable process, $\mathscr{Z}$ is smaller the larger is the delay. As consequence, the nominal control constraint, $\overline{\mathbb{U}}$, is larger. However, in the case of the nominal constraint on the state (output), it can be shown that $\overline{\mathbb{X}}$ gets smaller for longer delays only if the closed loop response is slower then open-loop one. In general ($b < a$), the longer is the delay, the larger is the prediction error bound which makes more difficult to guarantee state (output) constraints satisfaction.

3.5 Case study

A laboratory heater process case study will be presented in this section. In this system, it is desired to control the temperature in the outlet side of a tube. A constant air stream is used to transfer heat from the heater to the output of the tube where there is a thermistor. An input tension is used to adjust the power dissipated in the heater meanwhile an output tension is used to obtain the temperature information. Both input and output tensions have the same range ($0 \leq V_{in} \leq 10$ and $0 \leq V_{out} \leq 10$). In order to emulate input disturbances, the air stream flow can be manually modified. An simplified schematic diagram is presented in Fig. 3.3 where $y(k) = V_{out}(k)$, $u(k) = V_{in}(k)$ and the air flow affects $w(k)$.

In order to demonstrate the moderate level of computational demand using the multi-parametric solution [4], it is be used a sampling period of 50ms. In this case, the FOPDT model in the form

$$P(z) = \frac{0.0314}{z-0.9556} z^{-4}$$

was obtained after some least square identification tests based on pseudo random binary aleatory input sequences.

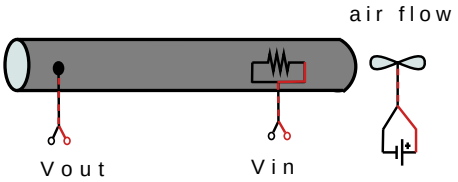

Figure 3.3: Simplified schematic representation of the heater process.

To guarantee robust stability and robust constraint satisfaction, it was defined that the disturbance bound for the delayed system is $\mathbb{W} \triangleq \{w| \, ||w||_\infty \leq 0.15\}$. The MPC tuning parameters are $Q = 1$, $R = 1$, $N = 5$ and $V_o(\bar{y}_s - y_t) = ||\bar{y}_s - y_t||_{100}$. The stabilizing elements K_Ω and P are obtained from the optimal solution of the unconstrained problem (linear quadratic solution) for (A, B, Q, R). Although there is a better strategy to choose K [22], for simplicity and similarly to [27], it is used $K_\Omega = K$. A second-order filter in the form

$$F(z) = \left(\frac{0.05z}{z - 0.95} \right)^2$$

is used in order to estimate the mean value of the disturbance, attenuating noise effect.

Simulated results with the nominal model are presented in Fig. 3.4. These results are useful to illustrate the robust tube idea: at each sampling instant, the optimal nominal value of the prediction ($\bar{y}^*(k+d|k)$), which may be different from the prediction ($y(k+d|k)$), is protected by an inner and an outer intervals. The smaller one would be enough to guarantee that $y(k+d|k)$ respect the constraints but, the larger one is imposed to ensure that the real future output respect the constraints. Due to the fact that it is considered $y(k+d|k)$ for control purposes, it is necessary to consider just the smaller interval to ensure control constraint satisfaction and recursive feasibility (robust stability).

Constant unmeasured disturbances are inserted in the control ($u_q = 4.5$ and $u_q = -3$), which corresponds to $w(k) = B * u_q$ as shown in Fig. 3.4(d). When $u_q = 4.5$, due to the constraints limits, the external limit of the tube reaches the lower constraint in such way that $\bar{y}^*(k+d|k)$ cannot be reduced which implies a steady-state error. Actually, off-set free could be achieved if the reference was set to a higher value, as 6 for instance, or if the disturbance were smaller as when $u_q = -3$. Some interesting points can be observed from Fig. 3.4(c). As $w(k)$ was close to one of its limits (0.15) for $u_q = 4.5$, the optimal solution was obtained with an active constraint in $\bar{x}_0 \in x \oplus (-\mathscr{Z})$. This can be verified because $\bar{y}^*(k+d|k)$ (alternatively $\bar{y}^*(k|k-d)$) is exactly over the border. As a consequence, the real output almost reached of its limits which illustrates that: i) this algorithm is not conservative in the case of constant disturbances and ii) constraint satisfaction may be violated if the external interval is not considered. Actually, the real output would reach the external border if $w(k) = 0.15$.

In the experimental results, disturbances were applied by varying the air stream flow manually. Apart from the noise effect, the results are somehow similar to the simulated case. It is interesting to observe that disturbance dynamics varied naturally during the process operation. Note, for instance, that when $w(k)$ is in the neighborhood of 800 samples it presents a different behavior from those in the neighborhood of 1500 samples despite the fact that the system is around the same equilibrium point. It is clear that this issue is not a problem for a robust algorithm since the limits for $w(k)$ were respected. It should be also noticed that disturbance variance changed during the process operation but this effect does not affect control signal due to the disturbance estimation filter. Moreover, constant disturbance rejection was properly performed as expected.

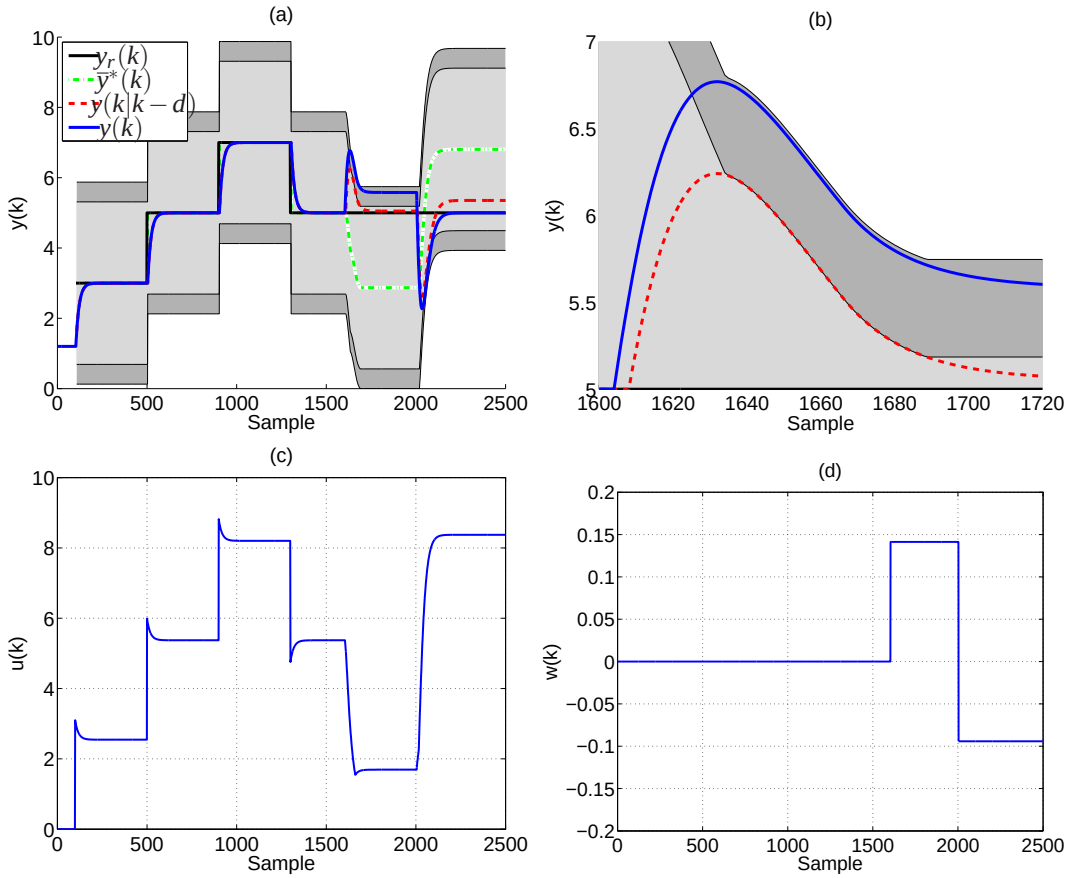

Figure 3.4: Simulated behavior of the nominal system: (a) output response, (b) detail of the output response, (c) control action and (d) additive disturbance.

3.6 Final remarks

In this chapter, the explicit compensation effect was discussed in a robust context. The conditions to guarantee robust stability and robust constraint satisfaction, in the presence of additive state disturbances, were presented. A robust tube MPC was applied to guarantee these conditions and a FOPDT model was considered to take some advantages of the proposed explicit compensation MPC scheme. Finally an experimental case study was used to discuss some properties of the proposed algorithm. As future work, it would be interesting to guarantee robust constraint satisfaction by using different explicit dead-time compensation schemes.

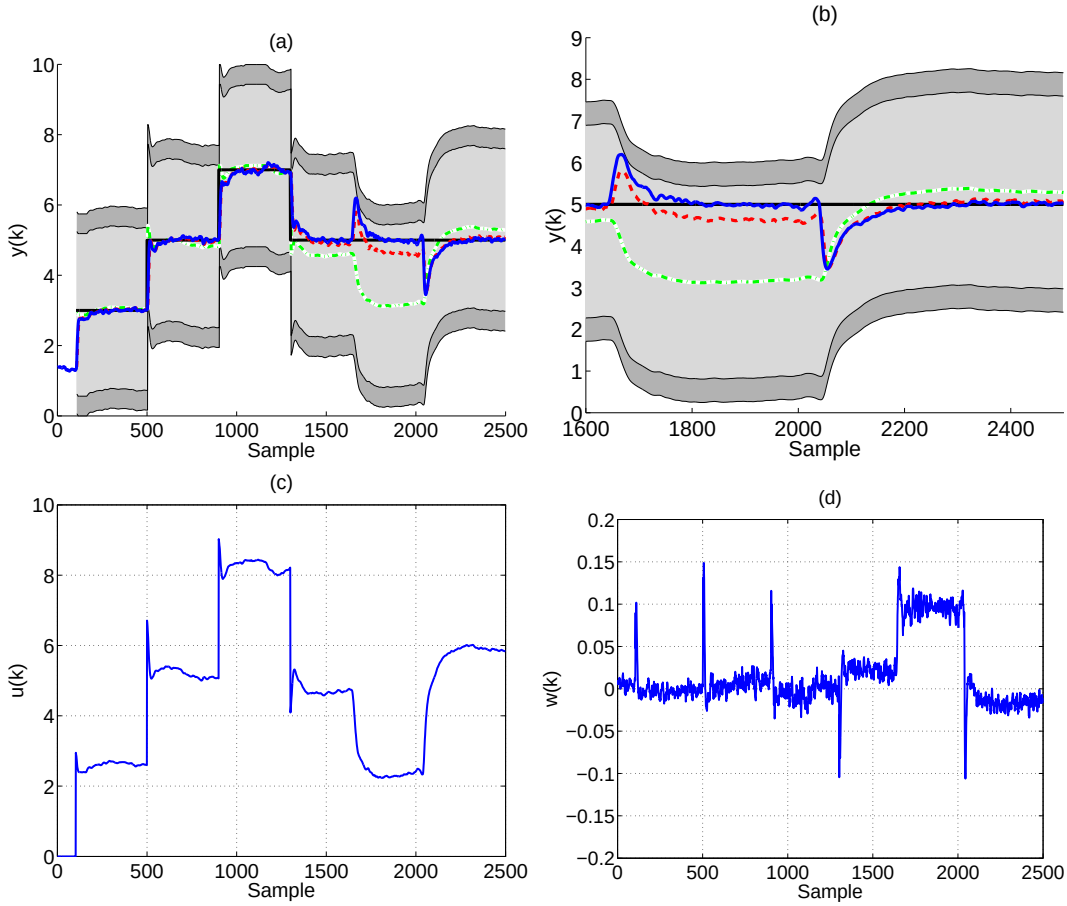

Figure 3.5: Experimental behavior of the real system: (a) output response, (b) detail of the output response, (c) control action and (d) additive disturbance. In (a) and (b), legends are the same of Fig. 3.4(a).

Chapter 4

Stability and Performance Analysis of Irrigation Channels with Distributed Control

4.1 Introduction

Water is becoming a scarce resource all over the world. Irrigation accounts for 70% of water usage [42]. Fig. 4.1 shows the top-view of a typical irrigation network. Water is drawn from the reservoir

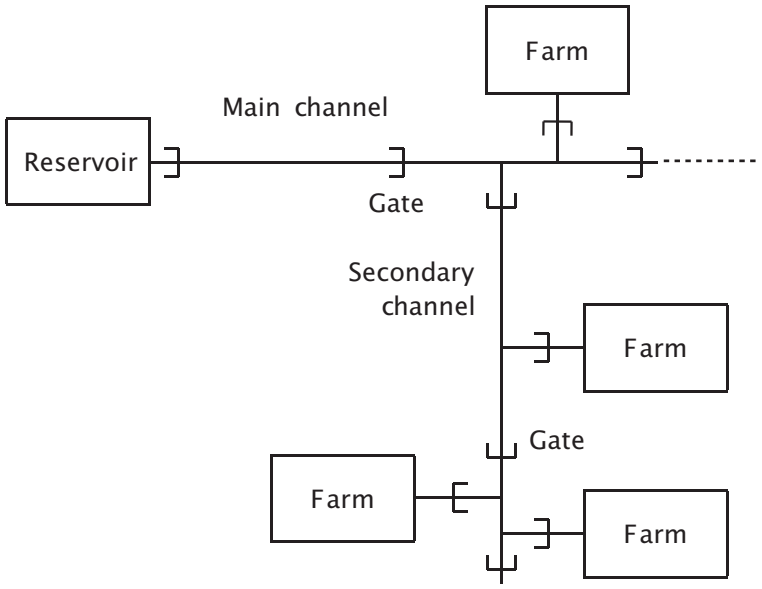

Figure 4.1: Top-view of an irrigation network

and distributed through the main channel and many secondary channels to farms. Along the channels, mechanical gates are installed to regulate the flow, as shown in Fig. 4.2. A stretch of water between two neighboring gates is called a pool. An irrigation network is largely gravity-fed (i.e. there is no pumping); to satisfy water-demands from farms and to decrease water wastage, the water-levels in the pools should be regulated to certain setpoints. Since most farms sit at the downstream ends of pools,

Figure 4.2: An irrigation channel (Source: Rubicon Systems Australia Pty. Ltd)

it is more important to control downstream water-levels. To avoid the excessive communication load for large-scale system, decentralized control is preferred to centralized control. In practice, a distant-downstream control structure (i.e. use upstream gate to control downstream water-level of a pool) is implemented for good management of water service and water distribution efficiency [24]. Further, an irrigation channel is a system presenting strong interactions between pools, i.e. the flow into a pool is equivalent to the flow out of the neighboring upstream pool. When off-takes occur at downstream pool, one could see amplification of the control action (e.g. flow over upstream gates) and water-level error propagation towards upstream, see [6, 21]. Therefore, control objectives for large-scale irrigation network involve: locally, setpoints regulation, rejection of off-take disturbances, avoiding excitement of dominant waves and, globally, management of the water-level error propagation and attenuation of the amplification of control action in the upstream direction. As shown in [21], there exists a tradeoff between the local and the global control performance. To cope with such a tradeoff, a distributed control scheme that inherits the interconnecting structure of the plant is suggested in [6, 20]. Such a distributed control scheme presents performance advantage over decentralized feedback with feed-forward control [44].

In fact, one big issue in control design for an irrigation network comes from the time-delay in each pool, i.e. the time for transporting water from the upstream gate to the downstream gate. In this paper, the impact of the internal time-delays on the local and global control performance is analyzed. Further, we discuss how the distributed control scheme compensates for such impact. Although the paper focuses on irrigation networks, the discussion can be extended to many practical networks that involve internal time-delay. The paper is organized as follows. Section 4.2 briefly introduces modeling of an irrigation channel and designing of the distributed controller. In Section 4.3, discussions are made on how the distributed control scheme manages the water-level error propagation and attenuates

the amplification of control actions in the upstream direction. Section 4.4 summarizes the paper.

4.2 Modeling of a channel and designing of distributed controller

Fig. 4.3 shows an irrigation channel with a special structured distributed control, i.e. the information flow is uni-directional: from controller K_{i+1} to controller K_i. When water off-takes occur in a pool, such an interconnection structure confines the water-level error propagation and amplification of control action in the upstream pools. Hence, such a control scheme avoids the requirement of water storage at the downstream end of the channel.

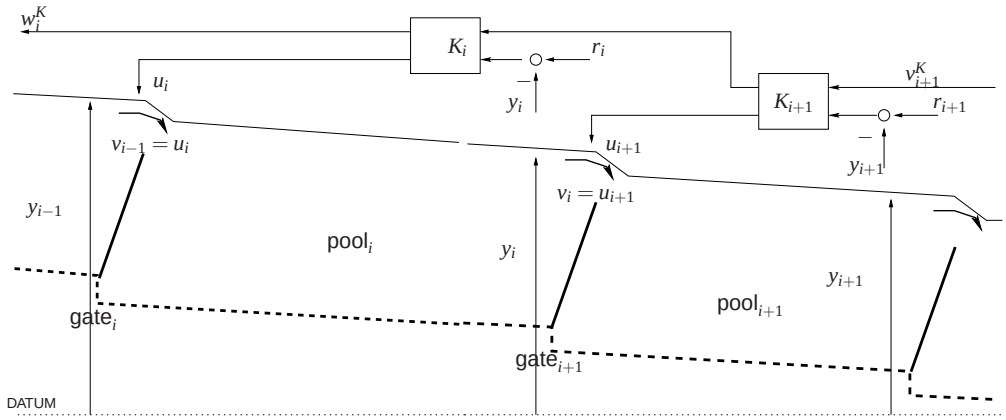

Figure 4.3: Distributed control of an open water channel

4.2.1 Plant model

A simple model of the water-level in pool$_i$ can be obtained by conservation of mass [6, 43]:

$$\alpha_i \dot{y}_i(t) = u_i(t-\tau_i) - v_i(t) - d_i(t),$$

where u_i is the flow over the upstream gate, v_i the flow over the downstream gate, d_i models the off-take load-disturbances from pool$_i$; τ_i is the transport delay of water from upstream gate to downstream gate of the pool, and α_i a measure of the pool surface area. Note the interconnection $v_i = u_{i+1}$, i.e. the flow out from pool$_i$ equals the flow into pool$_{i+1}$. Taking Laplace transform, yields

$$P_i : \; y_i(s) \;=\; \frac{1}{s\alpha_i}\left(e^{-s\tau_i}u_i - v_i - d_i\right)(s). \tag{4.1}$$

4.2.2 Designing of the distributed controller

Fig. 4.4 shows a localized portion of a channel under distributed distant-downstream control, where P_i is the nominal model (4.1) for pool$_i$, and K_i in Fig. 4.3 is split into a loop-shaping weight W_i and a compensator K_{∞_i} (with y_i^K and u_i^K, input from and output to the shaped plant, respectively). Note the constraint on the interconnection between controllers $v_i^K = w_{i+1}^K$. Designing of the distributed controller consists of the following three steps, which are consistent with the well-known $\mathscr{H}_\infty$ loop-shaping approach [28].

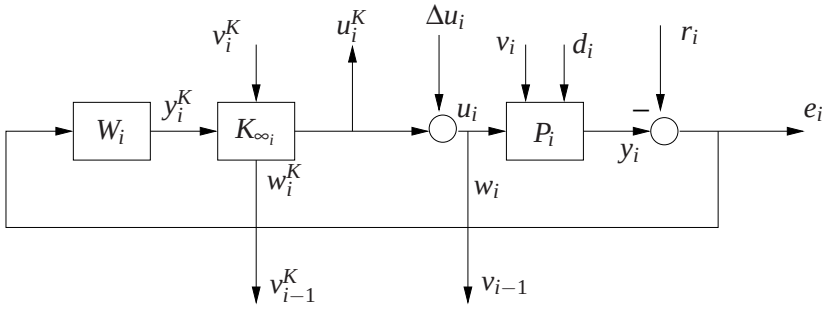

Figure 4.4: Localized portion of distributed controller design

1. Design W_i to shape P_i based on local performance. Typical off-takes d_i are step disturbances; based on the internal model principle [13], a simple selection could be $W_i = \frac{\kappa_i}{s}$ for zero steady-state water-level error. For robust stability, κ_i is selected such that the local crossover frequency $\omega_{c_i} \leq 1/\tau_i$ (see [40]). Denote $z_i := \left(e_i, u_i^K\right)^T$ and $n_i := (r_i, \Delta u_i, d_i)^T$, with r_i the water-level setpoint and Δu_i modeling additional uncertainty in flow over gate$_i$. For a channel of N pools, Let $G_s := (G_{s_1}, \ldots, G_{s_N})$ denote the interconnection of the shaped plant

$$
\begin{aligned}
G_{s_i} &:= \begin{pmatrix} v_i \\ n_i \\ u_i^K \end{pmatrix} \mapsto \begin{pmatrix} w_i \\ z_i \\ y_i^K \end{pmatrix} \\
&= \begin{bmatrix} 0 & (0\ 1\ 0) & 1 \\ \begin{pmatrix} \frac{1}{s\alpha_i} \\ 0 \end{pmatrix} & \begin{pmatrix} 1 & \frac{e^{-s\tau_i}}{-s\alpha_i} & \frac{1}{s\alpha_i} \\ 0 & 0 & 0 \end{pmatrix} & \begin{pmatrix} \frac{e^{-s\tau_i}}{-s\alpha_i} \\ 1 \end{pmatrix} \\ \frac{W_i}{s\alpha_i} & \begin{pmatrix} W_i & \frac{e^{-s\tau_i}W_i}{-s\alpha_i} & \frac{W_i}{s\alpha_i} \end{pmatrix} & \frac{e^{-s\tau_i}W_i}{-s\alpha_i} \end{bmatrix}
\end{aligned}
$$

   with $v_i = w_{i+1}$ and boundary condition $v_N = 0$. Note that such a boundary condition is possible with distant-downstream control.

2. Synthesize K_{∞_i} to cope with the tradeoff between local performance and closed-loop coupling.[1] Let $K_\infty := (K_{\infty_1}, \ldots, K_{\infty_N})$ denote the interconnection of

$$
K_{\infty_i} \quad := \quad \begin{pmatrix} v_i^K \\ y_i^K \end{pmatrix} \mapsto \begin{pmatrix} w_i^K \\ u_i^K \end{pmatrix}
$$

   with $v_i^K = w_{i+1}^K$ and boundary condition $v_N^K = 0$; and let $H(G_s, K_\infty)$ denote the closed-loop transfer function from $(n_1, \ldots, n_N)^T$ to $(z_1, \ldots, z_N)^T$. The synthesis problem is formulated as

$$
\begin{aligned}
&\min_{K_\infty \in \mathscr{K}_{\text{syn}}} \gamma \\
&\text{subject to} \\
&\|H(G_s, K_\infty)\|_\infty \ < \ \gamma
\end{aligned}
\tag{4.2}
$$

   where $\mathscr{K}_{\text{syn}}$ represents the set of stabilizing K_∞'s. Note that we use $\|\cdot\|_\infty$ to denote the $\mathscr{H}_\infty$ norm of a transfer function. Such a structured optimization problem can be solved by employing the technique in [19], see [20].

3. The final distributed controller is then given by

$$
K_i \quad := \quad \begin{pmatrix} v_i^K \\ e_i \end{pmatrix} \mapsto \begin{pmatrix} w_i^K \\ u_i \end{pmatrix} = K_{\infty_i} \begin{bmatrix} 1 & 0 \\ 0 & W_i \end{bmatrix}.
$$

[1] For local performance, one considers e_i to be small; while closed-loop coupling is cause by control action u_i to compensate e_i. As shown in [6, 21], for purely decentralized feedback control, $T_{r_i \mapsto e_i} + T_{d_i \mapsto u_i} e^{-s\tau_i} = 1$.

4.3 Closed-loop performance

For distant-downstream control, the internal time-delay τ_i limits the local performance. For example, the local bandwidth limit of $1/\tau_i$ is previously considered in the selection of the weight gain, κ_i. In this section, the influences of τ_i on the closed-loop coupling are discussed. It is shown that such time-delays, not only make it difficult to manage the water-level error propagation, but also cause the amplification of control action, in the upstream direction. Further, analysis is made on how the distributed control compensates for such influences.

4.3.1 The impact of τ_i on global closed-loop performance

From (4.1), for a channel of N pools

$$\begin{aligned}\begin{pmatrix} y_1 \\ \vdots \\ y_{N-1} \\ y_N \end{pmatrix} &= \begin{bmatrix} G_1 & \tilde{G}_1 & & \\ & \ddots & \ddots & \\ & & G_{N-1} & \tilde{G}_{N-1} \\ & & & G_N \end{bmatrix} \begin{pmatrix} u_1 \\ \vdots \\ u_{N-1} \\ u_N \end{pmatrix} \\ &+ \begin{bmatrix} \tilde{G}_1 & & \\ & \ddots & \\ & & \tilde{G}_N \end{bmatrix} \begin{pmatrix} d_1 \\ \vdots \\ d_N \end{pmatrix} \end{aligned} \tag{4.3}$$

where $G_i = \frac{1}{s\alpha_i} e^{-s\tau_i}$ and $\tilde{G}_i = -\frac{1}{s\alpha_i}$. As previously mentioned, it is reasonable to assume $v_N = 0$ as boundary condition for synthesis of the distributed controller under distant-downstream control. The distributed controller is represented by

$$\begin{aligned} K_1 &: u_1 = \begin{bmatrix} K_1^{21} & K_1^{22} \end{bmatrix} \begin{pmatrix} w_2^K \\ e_1 \end{pmatrix} \\ K_i &: \begin{pmatrix} w_i^K \\ u_i \end{pmatrix} = \begin{bmatrix} K_i^{11} & K_i^{12} \\ K_i^{21} & K_i^{22} \end{bmatrix} \begin{pmatrix} w_{i+1}^K \\ e_i \end{pmatrix} \\ &\quad \text{for } i = 2, \ldots, N-1 \\ K_N &: \begin{pmatrix} w_N^K \\ u_N \end{pmatrix} = \begin{bmatrix} K_N^{12} \\ K_N^{22} \end{bmatrix} e_N \end{aligned}$$

This gives the general form of the distributed controller K:

$$\begin{pmatrix} u_1 \\ \vdots \\ u_N \end{pmatrix} = \begin{bmatrix} K_{11} & \cdots & K_{1N} \\ & \ddots & \vdots \\ & & K_{NN} \end{bmatrix} \begin{pmatrix} e_1 \\ \vdots \\ e_N \end{pmatrix}; \tag{4.4}$$

where for $i = 1, \ldots, N$, $K_{ii} = K_i^{22}$, which takes care of local performance, and the additional decoupling terms

$$\begin{aligned} K_{i,i+1} &= K_i^{21} K_{i+1}^{12}, \\ K_{ij} &= K_i^{21} \left(\prod_{k=i+1}^{j-1} K_k^{11} \right) K_j^{12} \text{ for } j > i+1. \end{aligned} \tag{4.5}$$

Note that $e_i = r_i - y_i$. Then the closed-loop relationship between water-level errors and off-take disturbances is:

$$\begin{pmatrix} e_1 \\ \vdots \\ e_N \end{pmatrix} = \begin{bmatrix} M_{11} & \cdots & M_{1N} \\ & \ddots & \vdots \\ & & M_{NN} \end{bmatrix} \begin{pmatrix} d_1 \\ \vdots \\ d_N \end{pmatrix} \tag{4.6}$$

where for $i = 1, \ldots, N$, $M_{ii} = -\tilde{G}_i \left(1 + G_i K_{ii}\right)^{-1}$ and for $j \geq i+1$

$$M_{ij} \quad = \quad M_{ii} \sum_{k=i+1}^{j} \left(K_{i+1,k} - K_{ik} e^{-s\tau_i}\right) M_{kj}. \tag{4.7}$$

We see that the closed-loop transfer matrix is upper-triangular, hence the multivariable system inherits the local stabilities. That is, the multivariable system is stable *if and only if* all monovariable systems are stable. Since all the lower off-diagonal entries are null, even for model mismatch, robustness is also inherited from local systems. A perfect decoupling is achieved if for all $j > i$,

$$K_{i+1,j} - K_{ij} e^{-s\tau_i} = 0. \tag{4.8}$$

This requires $K_{ij} = K_{i+1,j} e^{s\tau_i}$, which is non-causal and hence impractical.

Next, analysis of global closed-loop performance is made on the two typical coupling properties of a (distant-downstream) controlled irrigation channel: water-level error propagation and amplification of control action. Assume only d_N occurs in the system, while $d_i = 0$ for $i = 1, \ldots, N-1$. Then from (4.6),

$$\begin{aligned}
&T_{e_{i+1} \mapsto e_i} := M_{i,N} M_{i+1,N}^{-1} \\
&= M_{ii}(K_{i+1,i+1} - e^{-s\tau_i} K_{i,i+1}) + \\
&M_{ii} \sum_{k=i+2}^{N} \left(K_{i+1,k} - K_{ik} e^{-s\tau_i}\right) M_{kN} \\
&\left(M_{i+1,i+1} \sum_{k=i+2}^{N} \left(K_{i+2,k} - K_{i+1,k} e^{-s\tau_{i+1}}\right) M_{kN} \right)^{-1}.
\end{aligned}$$

Small $\|T_{e_{i+1} \mapsto e_i}\|_\infty$ (e.g. $\ll 1$) represents a good management of the water-level error propagation.

Remark. 2 *For the case of a string of identical pools with purely decentralized feedback control (i.e. $K = \boldsymbol{diag}(K_{ii})$), $T_{e_{i+1} \mapsto e_i} = M_{ii} K_{i+1,i+1}$. If the selected K_{ii}'s are identical for all $i = 1, \ldots, N$, then $\|T_{e_{i+1} \mapsto e_i}\|_\infty > 1$ (see [6, 21]). Such a strategy, i.e. designing K_{ii} only based on local control performance, creates very strong coupling between loops (since $\|T_{e_{i+1} \mapsto e_i}\|_\infty$ occurs at the same frequency for all i). Instead, to decouple the interaction between pools, one can design K_{ii}'s such that the downstream closed-loop be slower than the upstream ones.*[2] *However, it is nontrivial to cope with the tradeoff between local performance and closed-loop decoupling by simply tuning the feedback controller. In contrast, the resulted distributed controller, by taking the three steps in Section 4.2, optimizes a measure of the global performance, accounting for such a tradeoff.*

From (4.4) and (4.6), the coupling of control actions responding to d_N is

$$T_{u_{i+1} \mapsto u_i} \quad := \quad \sum_{k=i}^{N} K_{ik} M_{kN} \left(\sum_{k=i+1}^{N} K_{i+1,k} M_{kN} \right)^{-1}.$$

The following discussion shows that $\|T_{u_{i+1} \mapsto u_i}\|_\infty > 1$.

For an irrigation channel with purely decentralized feedback control, i.e. K in (4.4) being diagonal, $T_{u_{i+1} \mapsto u_i} = M_{ii} K_{ii} = -\tilde{G}_i K_{ii} \left(1 - \tilde{G}_i K_{ii} e^{-\tau_i s}\right)^{-1}$. Note that $\tilde{G}_i K_{ii}$ involves two integrators.[3] Applying Lemma 9.3 of [13], it is straightforward to prove $\|T_{u_{i+1} \mapsto u_i}\|_\infty > 1$.

[2] Such a scheme is similar as the one suggested in [17] for the control of a platoon of vehicles, that string instability can be avoided at the expense of successively more aggressive control laws with linearly increasing gains.

[3] As previously discussed, for zero steady-state water-level error, an integrator is involved in K_{ii}.

i	τ_i	α_i	ψ_i
1	6 min	10344 m^2	0.349 rad/min
2	25 min	39352 m^2	0.084 rad/min
3	15 min	26317 m^2	0.140 rad/min

Table 4.1: Pool model parameters: delay (τ_i), surface area (α_i) and wave frequency (ψ_i)

Generally, under distant-downstream control (i.e. without the constraints that K in (4.4) be diagonal), to compensate the influence of the internal time-delay, the amplification of control action in the upstream direction is unavoidable. This is shown in Fig. 4.5. Initially, the system is at steady-state.

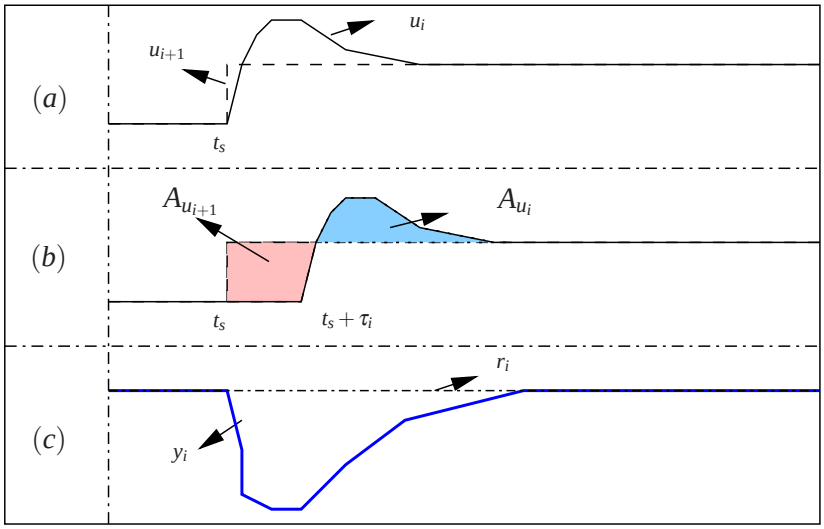

Figure 4.5: Control actions for zero steady-state water-level error

At time t_s, the flow out of pool$_i$ increases, see the change of u_{i+1} (the dashed line in Fig. 4.5(a)). To compensate for the influence of u_{i+1} on y_i, the flow into the pool, u_i, also increases (the solid line in Fig. 4.5(a)). However, the influence of u_i on the downstream water-level y_i will be τ_i(min) later than that of u_{i+1} on y_i (see Fig. 4.5(b)). For zero steady-state error of y_i from r_i (see Fig. 4.5(c)), from (4.1), u_i should be greater than u_{i+1} for some time such that the area of A_{u_i} is equivalent to the area of $A_{u_{i+1}}$. Hence, $\|T_{u_{i+1}\mapsto u_i}\|_\infty > 1$.

In Section 4.3.2, the analysis focuses on the impact of the decoupling terms in the distributed controller on the closed-loop performance.

4.3.2 The influence of K_{ij} ($j > i$) on closed-loop decoupling

As discussed in Section 4.2.2, the synthesis of K_∞ copes with the tradeoff between the local performance and the decoupling of the closed-loop system. To see how the distributed controller compensates for the influence of internal time-delays, we study the time and frequency responses of a string of three pools with distributed control.

The three pools are taken from Eastern Goulburn No 12, Victoria, Australia. Table I gives the identified model parameters [33]. To shape the plant, we choose $W_1 = \frac{87.206}{s}$, $W_2 = \frac{20.8865}{s}$, $W_3 =$

$\frac{32.6255}{s}$.[4] A $\gamma = 3$ is achieved by solving the structured optimization problem (4.2). The final controller is shown in Fig. 4.6. All the terms involve an integrator, which comes from the shaping weight. Note

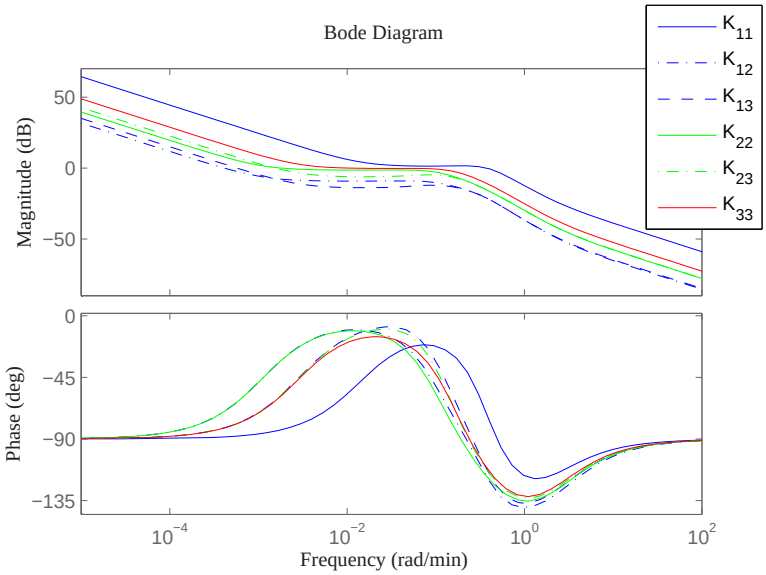

Figure 4.6: The distributed controller

that K_{12} has similar phase property as K_{22}, i.e. they both involve phase-lead-lag-lag-lead compensation around the same mid-frequency range; while K_{13}, K_{23} have similar phase property as K_{33}.

Fig. 4.7 shows the open loop-gain for $\text{pool}_{1,2,3}$. High gain at low frequency is obtained, with the bandwidths 0.0408 rad/min, 0.0085 rad/min and 0.0132 rad/min respectively. Around the wave frequencies, the loop-gains are around -20 dB, -20 dB and -25 dB respectively. This ensures no excitement of dominant waves in all the three pools.

From (4.5), K_{12} and K_{23} have a similar structure, while K_{13} involves K_2^{11} for decoupling. The following analysis is made by checking the impact of K_{23}[5] and K_{13} on decoupling of the closed-loop system.

Impact of K_{23}

The gains of $T_{d_3 \mapsto e_2}$ and $T_{d_3 \mapsto u_2}$, with and without K_{23}, are given in Fig. 4.8. With K_{23}, a lower gain in the mid-frequency range is achieved.

Fig. 4.9 shows that K_{23} helps in decreasing $|T_{e_3 \mapsto e_2}|$ and $|T_{u_3 \mapsto u_2}|$ at the low and middle-frequency range, where d_3 is significant. One can thus expect a good management of the water-level error propagation and attenuation of the amplification of control action with K_{23}.

The time response of the close-loop system is shown in Fig. 4.10 and 4.11. In the simulation, the water-level setpoints are set as $r_i = 10$ m, for $i = 1,2,3$. Note that τ_2 is much bigger than τ_3; such a combination, i.e. a long upstream pool with a short downstream pool, is difficult for managing the tradeoff between the local water-level error and the amplification of control action.[6] When an

[4] As formerly discussed, the weight gains are chosen to set the loop-gain bandwidth just below $1/\tau_i$ rad/min.

[5] Similar impact of K_{12} as that of K_{23} on the closed-loop decoupling can be expected and hence the analysis is omitted here.

[6] As previously discussed, to decouple the closed-loop system, one should try to make the downstream loop slower than the upstream loop.

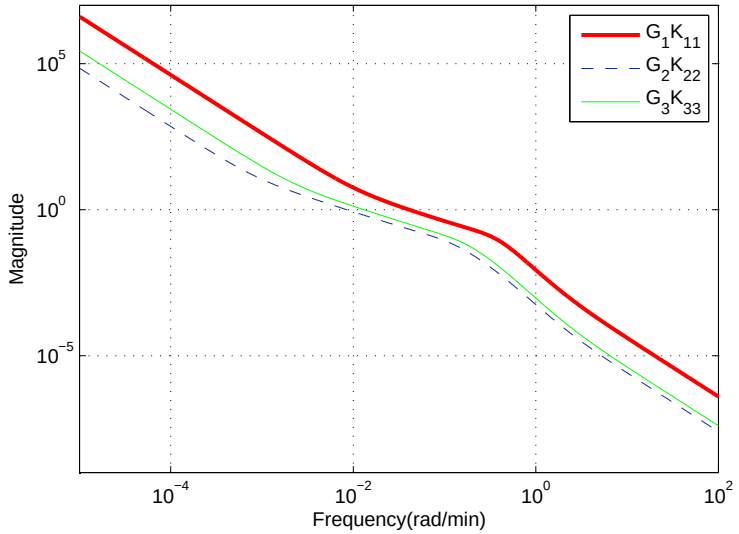

Figure 4.7: Local loop-gain with the distributed controller

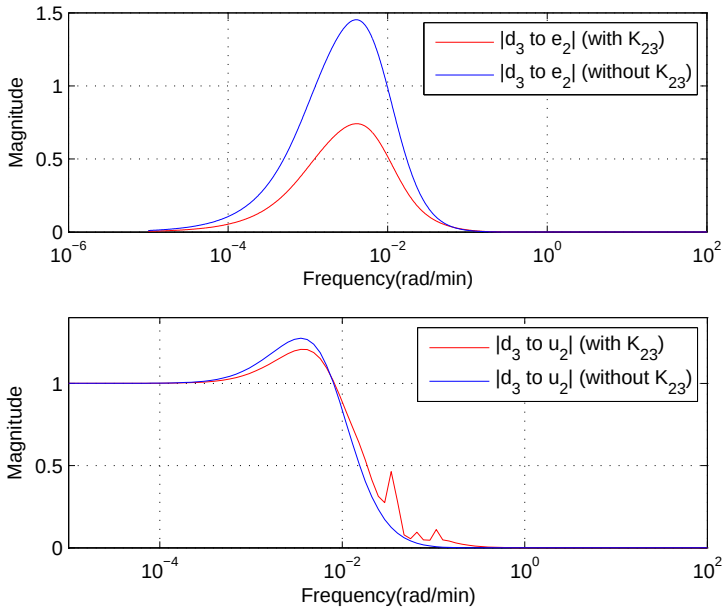

Figure 4.8: $|T_{d_3 \mapsto e_2}|$ (top) and $|T_{d_3 \mapsto u_2}|$ (bottom), with and without K_{23}

off-take of 98.6 Ml/day starts in pool_3 at 30 min till the end of the simulation scenario, the water-level error in pool_2 is better managed with K_{23} operating in the system than without K_{23}. Indeed, with K_{23}, $\max_t |e_2(t)|$ decreases about 0.08 m (compare the red solid line with the red dashed line). This is important since, as discussed in Section 4.1, in gravity-fed irrigation networks, water-levels represent the capacity to serve water-demands at the off-take points. Fig. 4.11 shows the upstream control actions in $\text{pool}_{2,3}$ to compensate the influence of d_3 on e_2 and e_3.[7] With K_{23}, u_2 responds to

[7]For clarity, we zoomed in to the first 1000 mins to show the changes of the control actions when d_3 starts. Note we did

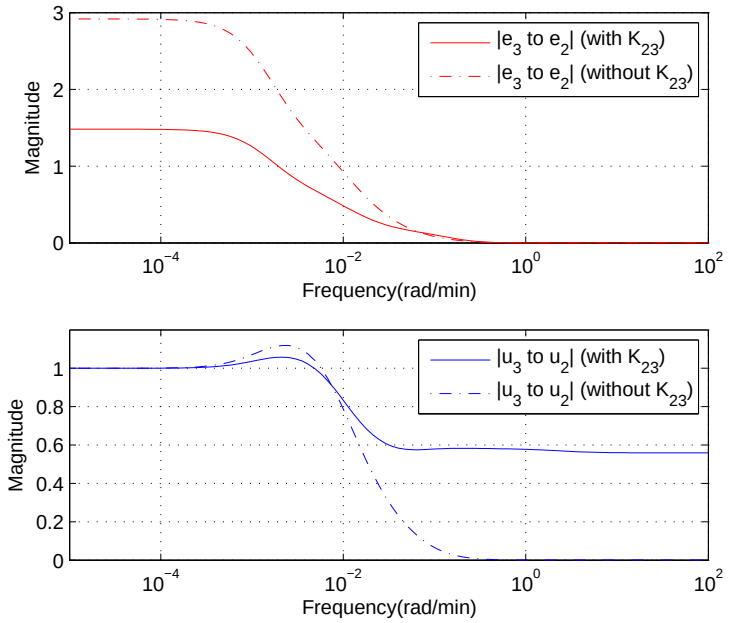

Figure 4.9: Closed-loop coupling: $|T_{e_3 \mapsto e_2}|$ and $|T_{u_3 \mapsto u_2}|$

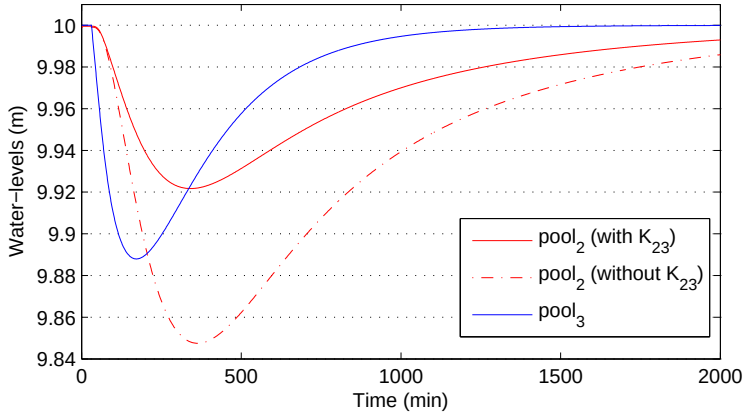

Figure 4.10: Water-level error propagation: with and without K_{23}

the change of u_3 faster than without K_{23} operating on the closed-loop. Note $\max_t |u_2(t)|$ is smaller with K_{23}, i.e. a better attenuation of the amplification of control action is obtained.

Impact of K_{13}

Fig. 4.12 shows $|T_{d_3 \mapsto e_1}|$ and $|T_{d_3 \mapsto u_1}|$, with and without K_{13}.[8] With K_{13}, a lower gain in the low and mid-frequency range is achieved, hence better decoupling of the closed-loop system can be expected. This is confirmed by the time responses shown in Fig. 4.13 and 4.14. When d_3 starts at 30 min, the water-level error in pool$_1$ is smaller with K_{13} (see the green solid line in Fig. 4.13) operating in the

the similar in Fig. 4.14.

[8] For the case of $K_{13} = 0$, it is assumed that $K_2^{11} = 0$, while K_{12} and K_{23} still operate on the closed-loop.

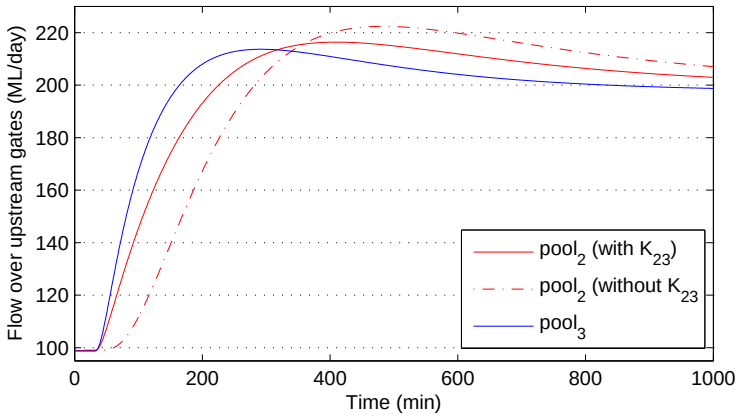

Figure 4.11: Amplification of control actions: with and without K_{23}

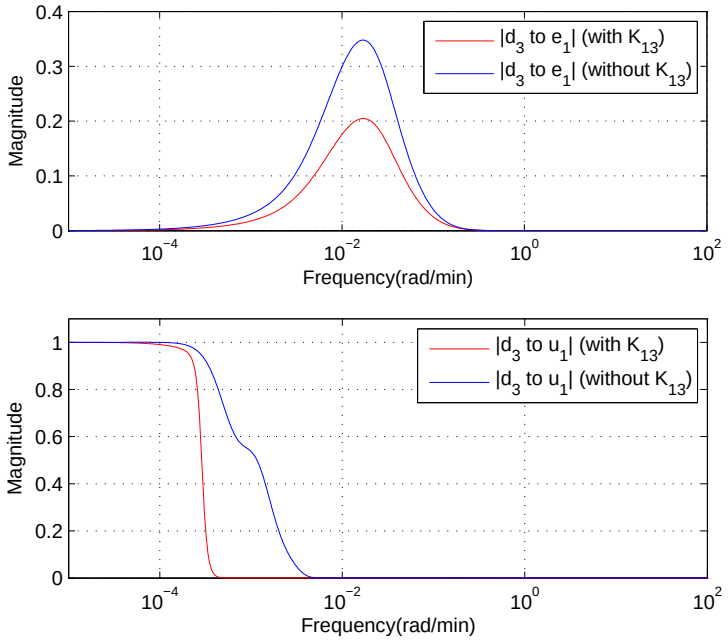

Figure 4.12: $|T_{d_3 \mapsto e_1}|$ (top) and $|T_{d_3 \mapsto u_1}|$ (bottom), with and without K_{13}

system than without K_{13} (the green dash-dot line). Fig. 4.14 shows the change of control actions in $\text{pool}_{1,2,3}$ in response to d_3. We see that with K_{13}, u_1 reacts faster to the change in u_2 than the case without K_{13}. Moreover, $\|u_1\|_\infty$ is smaller with K_{13}.

Some remarks

The closed-loop coupling term M_{ij} (see (4.7)) is composed of $M_{ij}^k := M_{ii}\left(K_{i+1,k} - K_{ik}e^{-s\tau_i}\right)M_{kj}$ for $k = i+1,\ldots,j$. Fig. 4.15 shows the impact of K_{ik} on M_{ij}^k in the above three-pool example. It is observed that

1. K_{ik} decreases the gain of M_{ij}^k at low frequencies where typical off-take disturbances are signifi-

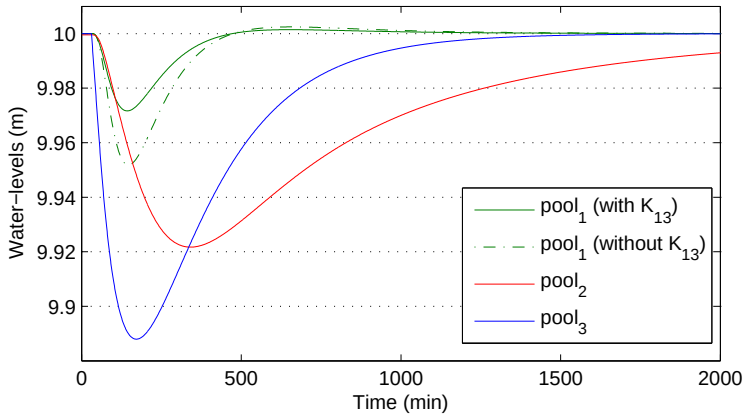

Figure 4.13: Water-level error propagation: with and without K_{13}

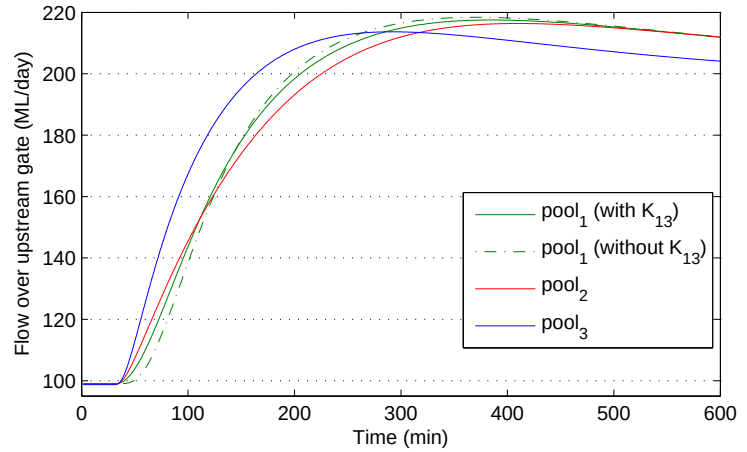

Figure 4.14: Control actions: with and without K_{13}

cant;

2. K_{ik} operates on M_{ij}^k by imposing on $M_{ii}K_{i+1,k}M_{kj}$ an additional phase lead-lag compensation around the frequency of $1/\tau_i$.

The first observation explains why with K_{ij} operating on the closed-loop, a better management of water-level error propagation is achieved (see Fig. 4.10 and 4.13). Although it is difficult to directly make conclusions of global performance from the second observation, time-responses of control actions (see Fig. 4.11 and 4.14) show that with the K_{ij}'s the closed-loop predicts the influence of the internal time-delays and that the control action in response to off-take disturbance is faster than that without the K_{ij}'s.

4.4 Summary

An irrigation channel is a system presenting strong interactions between pools. This paper considers distant-downstream control of irrigation channels. It is shown that the internal time-delay for trans-

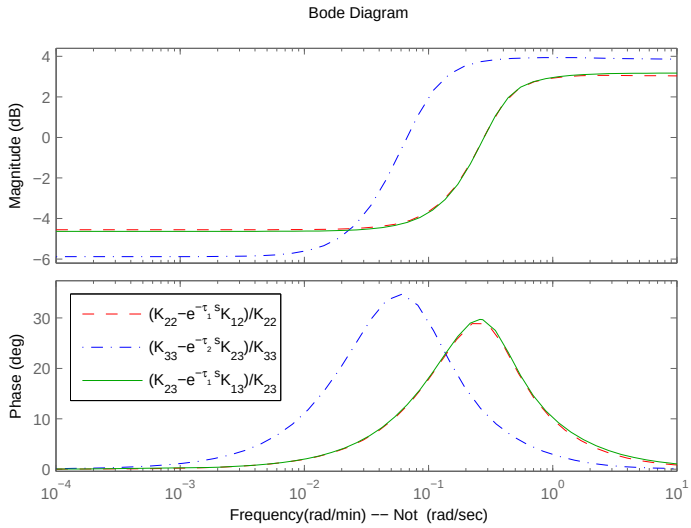

Figure 4.15: The decoupling function of K_{ik} for $k = i+1, \ldots, j$

portation of water from upstream to downstream of each pool not only limits the local performance, but also impacts the coupling between pools, i.e. the water-level error propagation and the amplification of control actions in the upstream direction. More specifically, we have discussed a distributed control that inherits the interaction structure of the plant. The controller is designed in a structured $\mathscr{H}_\infty$ loop-shaping approach. The involved optimization problem manages the tradeoff between local and global performance. Analysis shows that the distributed controller compensates the time-delay influence by decreasing the low-frequency gain of the close-loop coupling term and imposing extra phase lead-lag compensation in the mid-frequency range on the closed-loop coupling term.

Based on the above observations of the function of the decoupling terms of the distributed controller, it is of interest in future research to investigate the involvement of similar components, e.g. phase lead-lag in decentralized feed-forward compensators, in addition to the purely decentralized feedback controller, for a better global closed-loop performance.

Bibliography

[1] F. Allgöwer, T. A. Badgwell, S. J. Qin, J. B. Rawlings, and S. J. Wright. Nonlinear predictive control and moving horizon estimation - an introductory overview. In *Proceedings of the Advances in Control - Highlights of ECC '09*, pages 391–449, 1999.

[2] K. J. Åström and B. Wittenmark. *Computer-Controlled Systems*. Prentice Hall, Upper Saddle River, NJ, 1997.

[3] A. Bemporad, D. Mignone, and M. Morari. Moving horizon estimation for hybrid systems and fault detection. In *Proceedings of the American Control Conference*, pages 2471–2475, 1999.

[4] A. Bemporad, M. Morari, V. Dua, and E. N. Pistikopoulos. The explicit linear quadratic regulator for constrained systems. *Automatica*, 38(1):3 – 20, 2002.

[5] E. F. Camacho and C. Bordons. *Model Predictive Conrol*. Springer-Verlag, London, 2004.

[6] M. Cantoni, E. Weyer, Y. Li, S. K. Ooi, I. Mareels, and M. Ryan. Control of large-scale irrigation networks. *Proceedings of the IEEE*, Special Issue on the Technology of Networked Control Systems, 95(1):75–91, 2007.

[7] L. Chisci, J. A. Rossiter, and G. Zappa. Systems with persistent disturbances: predictive control with restricted constraints. *Automatica*, 37(7):1019 – 1028, 2001.

[8] M. Farina, G. Ferrari-Trecate, and R. Scattolini. Distributed moving horizon estimation for sensor networks. *IFAC Workshop on Estimation and Control of Networked Systems (NecSys'09)*, 2009.

[9] A. Ferramosca, D. Limon, I. Alvarado, T. Alamo, and E.F. Camacho. MPC for tracking with optimal closed-loop performance. *Automatica*, 45(8):1975 – 1978, 2009.

[10] K. Findeisen. Moving horizon state estimation of discrete-time systems. Master's thesis, University of Wisconsin-Madison, 1997.

[11] R. C. C. Flesch and J. E. Normey-Rico. Modelling, identification and control of a calorimeter used for performance evaluation of refrigerant compressors. *Control Engineering Practice*, 18(3):254 – 261, 2010.

[12] J. Garcia and J. Espinosa. Moving horizon estimators for large-scale systems. *Journal of Control Engineering and Applied Informatics -CEAI-*, 11(3):49–56, 2009.

[13] G. C. Goodwin, S. F. Graebe, and M. E. Salgado. *Control System Design*. Prentice Hall, Englewood Cliffs, NJ, 2001.

[14] G. C. Goodwin, H. Haimovich, D. E. Quevedo, and J. S. Welsh. A moving horizon approach to networked control system design. *Automatic Control, IEEE Transactions on*, 49(9):1427–1445, sep. 2004.

[15] N. Haverbeke, T. Van Herpe, M. Diehl, G. Van den Berghe, and B. De Moor. Nonlinear model predictive control with moving horizon state and disturbance estimation - application to the normalization of blood glucose in the critically ill. In *Proceedings of the 17th IFAC World Congress*, pages 9069–9074, 2008.

[16] K. H. Johansson, A. Horch, O. Wijk, and A. Hansson. Teaching multivariable control using the quadruple-tank process. In *Proceedings of the 1999 IEEE Conference on Decision and Control*, Phoenix, AZ, 1999.

[17] M. E. Khatir and E. J. Davidson. Bounded stability and eventual string stability of a large platoon of vehicles using non-identical controllers. In *Proceedings of IEEE CDC*, pages 1111–1116, 2004.

[18] I. Kolmanovsky and E. G. Gilbert. Theory and computation of disturbance invariant sets for discrete-time linear systems. *Mathematical Problems in Engineering:Theory, Methods and Applications.*, 4(4):317–367, 1998.

[19] C. Langbort, R. Chandra, and R. D'Andrea. Distributed control design for systems interconnected over an arbitrary graph. *IEEE Transactions on Automatic Control*, 49(9):1502–1519, 2004.

[20] Y. Li and M. Cantoni. Distributed controller design for open water channels. In *Proceedings of the 17th IFAC World Congress*, pages 10033–10038, Seoul, Korea, July 2008.

[21] Y. Li, M. Cantoni, and E. Weyer. On water-level error propagation in controlled irrigation channels. In *Proceedings of the 44th IEEE CDC*, pages 2101–2106, Seville, Spain, December 2005.

[22] D. Limon, I. Alvarado, T. Alamo, and E.F. Camacho. Robust tube-based MPC for tracking of constrained linear systems with additive disturbances. *Journal of Process Control*, 20(3):248 – 260, 2010.

[23] D. Limon, J. Espinosa, F. Valencia, J. Garcia, I.J. Wolf, W. Marquardt, and A. Nunez. Deliverable D3.4.1: Report of literature survey and analysis regarding timing and delay issues. Technical report, European FP7 STREP project HD-MPC, March 2010.

[24] X. Litrico and V. Fromion. Advanced control politics and optimal performance for an irrigation canal. In *Proceedings of the 2003 ECC*, Cambridge, UK, 2003.

[25] D. Q. Mayne, S. V. Rakovic, R. Findeisen, and F. Allgower. Robust output feedback model predictive control of constrained linear systems. *Automatica*, 42(7):1217–1222, Jul. 2006.

[26] D. Q. Mayne, J. B. Rawlings, C. V. Rao, and P. O. M. Scokaert. Constrained model predictive control: Stability and optimality. *Automatica*, 36(6):789 – 814, 2000.

[27] D. Q. Mayne, M. M. Seron, and S. V. Rakovic. Robust model predictive control of constrained linear systems with bounded disturbance. *Automatica*, 41(2):219–224, Fev. 2005.

[28] D. C. McFarlane and K. Glover. *Robust Controller Design Using Normalized Coprime Factor Plant Descriptions*. Lecture Notes in Control and Information Sciences. Springer-Verlag, 1990.

[29] H. Michalska and D. Q. Mayne. Moving horizon observers and observer-based control. *Automatic Control, IEEE Transactions on*, 40(6):995–1006, jun. 1995.

[30] J. E. Normey-Rico and E. F. Camacho. *Control of Dead-time Processes*. Springer-Verlag, London, 2007.

[31] J.E. Normey-Rico and E.F. Camacho. Multivariable generalised predictive controller based on the smith predictor. *Control Theory and Applications, IEE Proceedings* -, 147(5):538–546, Sept. 2000.

[32] S. Olaru and S.-I. Niculescu. Predictive control for linear systems with delayed input subject to constraints. In *Proceedings of the XVII IFAC Triennial Congress*, 2008.

[33] S. K. Ooi, M. Krutzen, and E. Weyer. On physical and data driven modeling of irrigation channels. *Control Engineering Practice*, 13(4):461–471, 2001.

[34] S.V. Rakovic, E.C. Kerrigan, K.I. Kouramas, and D. Q. Mayne. Invariant approximations of the minimal robust positively invariant set. *IEEE Transactions on Automatic Control*, 50(3):406–410, Mar. 2005.

[35] C. V. Rao, J. B. Rawlings, and D. Q. Mayne. Constrained state estimation for nonlinear discrete-time systems: Stability and moving horizon approximations. *IEEE Transactions on Automatic Control*, 48:246–258, 2003.

[36] C. V. Rao, S. J. Wright, and J. B. Rawlings. Application of interior-point methods to model predictive control. *Journal of Optimization theory and applications*, 99(3):723–757, 1998.

[37] C.V. Rao. *Moving Horizon Strategies for the Constrained Monitoring and Control of Nonlinear Discrete-Time Systems*. PhD thesis, University of Wisconsin-Madison, 2000.

[38] T. L. M. Santos, D. Limon, T. Alamo, and J. E. Normey-Rico. Robust tube based model predictive control for constrained systems with dead-time. In *Proceedings of the UKACC International Conference on Control (accepted for publication)*, 2010.

[39] T. L. M. Santos, D. Limon, J. E. Normey-Rico, and T. Alamo. On the explicit dead-time compensation in robust model predictive control. *Journal of Process Control*, Submitted, 2010.

[40] S. Skogestad and I. Postlethwaite. *Multivariable Feedback Control*. John Wiley and Sons, Chichester, UK, 1996.

[41] O. J. M. Smith. Closer control of loops with dead-time. *Chemical Engeneering Progress*, 53(5):217–219, 1957.

[42] UNESCO water report. The united nations world water development report, 2003. http://www.unesco.org/water/wwap.

[43] E. Weyer. System identification of an open water channel. *Control Engineering Practice*, 9(12):1289–1299, 2001.

[44] E. Weyer. Control of irrigation channels. *IEEE Transactions on Control Systems Technology*, 16(4):664–675, July 2008.

[45] J. K. Yook, D. M. Tilbury, and N. R. Soparkar. A design methodology for distributed control systems to optimize performance in the presence of time delay. *International Journal of Control*, 74(1):58–76, 2001.